packed with ODS (Fuji Silysia Chemical Ltd., Aichi, Japan), flow: 1 ml min^{-1}, column temperature: 50°C, injection volume: 20 µl, mobile phase: 55% acetonitrile/water, detection: UV (360 nm).

Standard aerobic plate count

A water sample (100 ml) was filtered through a membrane filter (0.22 µm) under reduced pressure. The filter was then placed upon a tryptone glucose yeast extract agar medium plate. The plates were incubated aerobically at 37°C for 24 h. Colonies were counted and expressed as colony forming unit (CFU) ml^{-1}.

Direct counting of bacteria with fluorescent staining

A water sample (50 ml) was drawn through a carbon membrane filter under negative pressure. The carbon membrane filter was strained by LIVE/DEAD BacLight bacterial viability kit, 1 ml stains mixture prepared according to the manufacture's instructions, and incubated for 20 min in the dark at room temperature. The mixture was removed and filters mounted with low-fluorescence immersion oil on glass microscope slides and observed by epifluorescence microscopy. The number of green cells was counted after viewing 20 microscopic fields.

ATP-based bioluminescent assay

The ATP derived from bacteria was measured by following methods. A 1 ml aliquot of water sample was placed in a tube, an ATP-eliminating reagent (0.1 ml) was added, the solution was mixed and it was incubated for 10 min to remove any extracellular ATP. A total of 0.1 ml of the solution then combined with 0.1 ml of a detergent for lysing cells before the addition of 0.1 ml luciferin-luciferase reagent. The sample was mixed and the amount of bioluminescence measured using a luminometer. The luminescence curves were prepared using the ATP standard solutions (2×10^{-12}–2×10^{-9} mol ml^{-1}). The results are expressed as relative light units (RLU) and ATP concentration.

Heterotrophic plate counting method

Heterotrophic plate counts (HPC) were obtained by plating 100 µl of tenfold dilutions of commercial water samples on R2A agar plates. The plates were incubated aerobically at 22°C for 72 h. Colonies were counted and the arithmetic mean expressed as CFU ml^{-1}.

Result

Analytical procedure

FA and AA in the PET bottle material were measured as described (Mutsuga et al. 2003, 2005). Recoveries of 76.9–101.2% were obtained for a PET pellet sample (0.5 g) spiked with FA (2.5 µg) and AA (2.5 µg). The limits of detection of FA and AA were 0.2 µg g^{-1} for each, based on the linearity of the calibration curve.

The analytical method for FA and AA in the commercial water was improved upon, and recovery rates of 85.7–104.9% were obtained for sterilized water (100 ml) spiked with FA and AA (1 and 10 µg each). The limit of detection of FA and AA were 5.0 µg l^{-1} for each, based on three times the blank value (FA: 1.34 ± 0.11 µg l^{-1} and AA: 0.77 ± 0.04 µg l^{-1}).

Contents of FA and AA in mineral water

The levels of FA and AA in the 20 commercial water samples are shown in Table I. FA and AA ranged from not detected (n.d.) to 27.9 µg l^{-1} and n.d. to 107.8 µg l^{-1}, respectively. All samples bottled in Japan had detectable levels of FA (10.1–27.9 µg l^{-1}) and AA (44.3–107.8 µg l^{-1}). In the European water, three samples had detectable levels of FA (7.8–13.7 µg l^{-1}) and AA (37.2–46.9 µg l^{-1}), while the remaining eight did not. In the North American water, two samples contained FA (13.6 and 19.5 µg l^{-1}) and AA (41.4 and 44.8 µg l^{-1}), while one did not. Most of the samples bottled in Europe and North America contained FA and AA under the detection limits. The detected levels of FA and AA in the Japanese water were higher than in the European or North American samples. There was no relationship between FA-and-AA content and pH or hardness of the commercial water. The samples were classified into two groups: those in which FA and AA were detected in the water (group A), those in which FA and AA were not detected in the water (group B). Group A contained all the sterilized water samples and three carbonated water samples. Group B contained unsterilized water samples without carbonate and one carbonated water sample.

Content of FA and AA in the bottle material and their migration

The levels of FA and AA in the bottle materials were analysed (Table I). The FA and AA levels of the Japanese bottles ranged from 1.3 to 2.9 µg g^{-1} and from 11.5 to 25.0 µg g^{-1}, respectively, while the European and North American bottles ranged from n.d. to 1.6 µg g^{-1} and from 5.2 to 17.1 µg g^{-1}, respectively. The levels of FA and AA in the Japanese bottles were significantly higher than that in European and North American bottles. The explanation for this may be the higher moulding temperatures used in the production of Japanese bottles (thicker bottle walls) and the use of scavengers in European bottles, which minimizes the

Table I. Contents of FA and AA in mineral water.

Region	Sample number	Bottled country	Representation				Bottle colour	Bottle material ($\mu g\,g^{-1}$)		Water ($\mu g\,l^{-1}$)		
			pH	Hardness	Sterilized	Carbonate		Formaldehyde	Acetaldehyde	Formaldehyde	Acetaldehyde	Classification
Japan												
	J-1	Japan	7.4	84	sterilized	–	colorless	2.2	16.7	10.1	44.3	group A
	J-2	Japan	8.3	32	sterilized	–	colorless	2.9	12.1	27.9	60.7	group A
	J-3	Japan	–	30	sterilized	–	colorless	1.6	13.6	15.0	41.1	group A
	J-4	Japan	–	99	sterilized	–	colorless	1.3	25.0	10.6	107.8	group A
	J-5	Japan	–	25	sterilized	–	colorless	2.4	14.0	15.4	66.3	group A
	J-6	Japan	7.1	28	sterilized	–	colorless	1.7	11.5	17.6	46.4	group A
Europe												
	E-1	France	7.0	62	not treated	–	pale blue	n.d.	8.8	n.d.	n.d.	group B
	E-2	France	7.3	309	not treated	–	colorless	1.0	5.5	n.d.	n.d.	group B
	E-3	France	7.2	294	not treated	–	colorless	0.7	7.2	n.d.	n.d.	group B
	E-4	France	7.6	628	not treated	–	colorless	0.7	5.4	n.d.	n.d.	group B
	E-5	France	–	201	not treated	carbonated	green	0.9	6.7	n.d.	n.d.	group B
	E-6	Italy	7.8	161	not treated	carbonated	deep blue	0.6	5.2	7.9	37.2	group A
	E-7	Italy	7.5	740	not treated	carbonated	green	0.9	8.4	13.7	37.8	group A
	E-8	Italy	5.8	609	not treated	carbonated	green	0.5	6.7	7.8	46.9	group A
	E-9	Italy	7.8	161	not treated	–	green	1.0	5.7	n.d.	n.d.	group B
	E-10	UK	–	104	not treated	–	colorless	1.6	7.5	n.d.	n.d.	group B
	E-11	UK	7.8	122	not treated	–	colorless	1.1	5.9	n.d.	n.d.	group B
North America												
	A-1	Canada	–	24	sterilized	–	pale blue	0.9	9.8	13.6	41.4	group A
	A-2	Canada	–	1	–	–	deep blue	n.d.	9.2	n.d.	n.d.	group B
	A-3	USA	–	38	sterilized	–	colorless	1.1	17.1	19.5	44.8	group A

–, No description.
Each value is the mean of three trials.
Bottle material n.d. $< 0.2\,\mu g\,g^{-1}$, water n.d. $< 5.0\,\mu g\,L^{-1}$.

Table II. Migration of FA and AA from PET bottles into water at 40°C.

Bottle	Contents in bottle ($\mu g\,g^{-1}$)		Storage days	Migration level ($\mu g\,l^{-1}$)	
	FA	AA		FA	AA
J-1	2.2	16.7	14	42.6	112.0
			30	55.2	169.6
E-1	0.7	5.4	14	11.4	14.5
			30	14.9	21.1

Each value is the mean of four trails

formation of FA and AA. Some of the bottles were blue or green colour. However, the results for the European bottles showed that the colour of bottles did not affect the FA and AA levels.

Migration tests were performed using Japanese (J-1) and European (E-1) bottles, in which J-1 bottle contained FA and AA while the E-1 bottles did not. The bottles were washed with sterilized water, then 100 ml sterilized water added, and stored at 40°C for 14 and 30 days. The analysis showed that migration of FA and AA occurred from both bottles to water (Table II). The migration levels of FA and AA depended on the level in the bottle material and duration of storage. Thus, the FA and AA in commercial water was a result of migration from their PET bottles.

Clarification of the disappearance of FA and AA in commercial water

The E-1 bottle showed migration of FA and AA into the sterilized test water, although the commercial water contained in the E-1 bottle was not contaminated with either FA or AA. Thus, it was speculated that unsterilized water might have some capacity to reduce levels of FA and AA.

Thus, 100 ml commercial water samples were transferred to a 200-ml glass bottle with plastic screw cap. Water samples were fortified with 2 μg FA and 10 μg AA and stored in the dark at 37°C for 48 or 96 h (Figure 1 and Table III). Figure 1 shows the time–response curves of FA and AA in E-1 and J-1 water for 12, 24, 36 and 48 h. In E-1 water, FA and AA reduced quickly and reached the 'blank' level after 48 h incubation, whereas the FA and AA in the J-1 water did not decline. Table III shows the recoveries of fortified FA and AA in several kinds of commercial water. Water of group B was able to reduce spiked FA and AA, while water of group A could not. Two carbonated water (E-6 and E-7) produced a small reduction in FA, and it seemed to be more volatile in carbonated water than still water at 37°C. However, water samples (E-1–3)

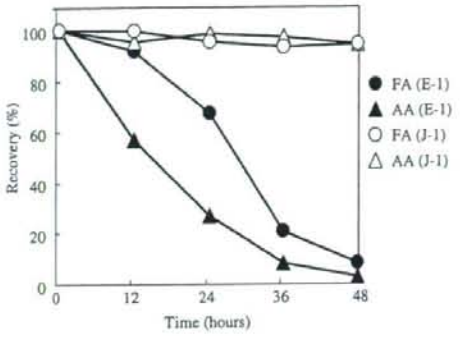

Figure 1. Recovery of FA (2 μg) and of AA (10 μg) fortified to 100 ml E-1 and J-1 water stored at 37°C. Each value is the means of two trials.

Table III. Recoveries of fortified FA and AA in several mineral water samples.

	Sample number	Incubation time (h)	Recovery (%)	
			Formaldehyde	Acetaldehyde
Group A	J-1	48	>95	>95
	J-1	96	>95	>95
	J-3	48	>95	>95
	J-6	48	>95	>95
	E-6	48	78	>95
	E-7	48	83	>95
	A-3	48	95	>95
Group B	E-1	48	<5	<5
	E-2	48	>95	75
	E-2	96	27	<5
	E-3	48	86	5
	E-5	48	>95	10
Sterilized group B	E-1	48	>95	>95
	E-2	96	>95	92
	E-3	48	>95	>95

FA (2 μg) and AA (10 μg) were added to 100 ml mineral water and stored at 37°C for 48 or 96 h.
Each value is the mean of two trials.

after sterilization in group B did not have the same ability to reduce levels.

According to these results, unsterilized commercial water can reduce the levels of FA and AA in the water. It is suspected that bacteria in commercial water were involved in the reduction in FA and AA.

Confirmation of bacterial activity

At first, the standard aerobic plate count method was performed. However, none of the water samples produced colonies. Therefore, the direct counting method was performed using the LIVE/DEAD BacLight bacterial viability kit, which contained two nucleic acid-binding stains, SYTO 9 and propidium iodide (Venkateswaran et al. 2003). SYTO 9 stained

Table IV. Amount of intracellular ATP in water.

Sample number	Bioluminescent assay: Luminescence (RLU)	Bioluminescent assay: ATP ($\times 10^{-11}$ M)	HPC assay colony count (CFU ml^{-1})
Group A			
J-1	n.d.*1	n.d.	n.d.*2
J-2	n.d.	n.d.	–
J-3	n.d.	n.d.	n.d.
J-4	n.d.	n.d.	–
J-5	n.d.	n.d.	–
J-6	n.d.	n.d.	–
E-6	n.d.	n.d.	n.d.
E-7	n.d.	n.d.	–
E-8	n.d.	n.d.	n.d.
A-1	n.d.	n.d.	–
A-3	n.d.	n.d.	–
Group B			
E-1	1005	14.3	1.5×10^5
E-2	149	1.9	3.2×10^4
E-3	801	11.3	7.8×10^4
E-4	655	9.2	–
E-5	1059	15.0	1.6×10^5
E-9	112	1.4	–
E-10	1003	14.2	4.1×10^4
E-11	3808	54.8	–
A-2	778	11.0	–

n.d.*1 < 100 RLU.
n.d.*2 < 100 CFU ml^{-1}.
Each value is the mean of three trials.
–, Not evaluated.

all cells green, while propidium iodide stained all the cells with damaged membranes red. As observed by epifluorescence microscopy, both viable and dead bacteria were detected. In J-1 water, neither green nor red bacteria were detected. On the other hand, in E-1 water, viable green bacteria were visualized (5×10^4 cells ml^{-1}). This bacterium was presumed to heterotrophic bacterium, which exists widely in the environment, as this bacterium is very small and there have been some reports documenting its existence in commercial water (Mosso et al. 1994; Tsai and Yu 1997; Ramalho et al. 2001; Leclerc and Moreau 2002).

Subsequently, intracellular ATP was measured by the ATP-based bioluminescent assay (Table IV). This method confirmed that none of the water samples in group A contained intracellular ATP. On the other hand, the water in group B showed intracellular ATP concentrations of between 1.4×10^{-11} and 5.5×10^{-10} M. Among the carbonated waters, intracellular ATP was detected in E-5 of group B, but not in E-6–8 of group A. All samples showed correlation between the existence of intracellular ATP and a reduction in FA and AA levels.

The enumeration of heterotrophic bacteria in the commercial mineral water is usually performed using the HPC method (Mosso et al. 1994; Tsai and Yu 1997; Ramalho et al. 2001; Leclerc and Moreau 2002; Venkateswaran et al. 2003). This method was recommended by Council Directive 98/83/EC (1998) for the count of heterotrophic bacteria in commercial water, and was performed in the present study on nine water samples by incubation for 72 h at 22°C on R2A medium. None of the water samples in group A possessed heterotrophic bacteria, while the water samples in group B formed between 1.6×10^3 and 1.5×10^5 CFU ml^{-1}.

Discussion

It has been shown that FA and AA migrated into commercial water from the PET bottle material. In commercial water without bacteria, the levels of migrated FA and AA remain unchanged, whereas in natural mineral water containing heterotrophic bacteria, the migrated FA and AA was decomposed. Of the carbonated water samples, one sample contained bacteria and showed a reduction in FA and AA, while the others had no bacteria and showed no decomposition activity. It was speculated that the existence of bacteria influenced the concentration of carbonate gas.

In the European Union regulations, natural mineral water cannot be treated for the elimination of microorganisms by disinfection or sterilization. The current drinking water guidelines in many European countries are based on recently revised Directive 98/83/EC. The current recommended microbiological standards include HPC limits for private supplies, i.e. no significant increase over normal levels when incubated at 22 and 37°C, and for bottled water within 12 h of bottling, 100 CFU ml^{-1} when incubated at 22°C for 72 h and 20 CFU ml^{-1} when incubated at 37°C for 48 h. In the present study, several European waters contained 1.6×10^3–1.5×10^5 CFU ml^{-1} heterotrophic bacteria. These waters appear to have passed the regulations during the bottling stage, but then bacteria proliferated during transport to Japan.

The potential negative impact to human health from the consumption of treated water containing high HPC levels of bacteria is still being debated. However, until now, no report has documented the decomposition of FA and AA by heterotrophic bacteria. PET bottled commercial water has two problems: the existence of heterotrophic bacteria and the migration of FA and AA, and the close relationship exists between these problems. Thus, it is

necessary to pay sufficient attention to both problems.

References

Council Directive 98/83/EC, on the quality of water intended for human consumption. Official Journal of the European Communities L330:32–54.

Dabrowska A, Borcz A, Nawrocki J. 2002. Aldehyde contamination of mineral water stored in PET bottles. Food Additives and Contaminants 20:1170–1177.

Dong M, DiEdwardo HA, Zitomer F. 1980. Determination of residual acetaldehyde in polyethylene terephthalate bottles, preforms, and resins by automated headspace gas chromatography. Journal of Chromatographic Science 18:242–246.

Duflos J, Leroy C, Gervais B, Dupas G, Bourguignon J, Queguiner G. 1993. Analysis of residual acetaldehyde and formaldehyde in PET via HPLC. Analusis 21:313–317.

Ewender J, Franz R, Mauer A, Welle F. 2003. Determination of the migration of acetaldehyde from PET bottles into non-carbonated and carbonated mineral water. Deutsche Lebensmittel-Rundschau 99:215–221.

Hirayama T, Kashima A, Watanabe T. 2003. Amounts of formaldehyde in tap water and commercially available mineral water. Journal of the Food Hygienics Society of Japan 10:138–144.

Leclerc H, Moreau A. 2002. Microbiological safety of natural mineral water. FEMS Microbiology Reviews 26:207–222.

Linssen J, Reitsma H, Cozijnsen J. 1995. Static headspace gas chromatography of acetaldehyde in aqueous foods and polyethylene terephthalate. Zeitschrift für Lebensmittel-Untersuchung und- Forschung 201:253–255.

Mosso AM, Rosa CM, Vivar C, Medina M. 1994. Heterotrophic bacterial populations in the mineral water of thermal springs in Spain. Journal of Applied Bacteriology 77:370–381.

Mutsuga M, Kawamura Y, Tanamoto K. 2003. Analytical method for formaldehyde, acetaldehyde and PET cyclic oligomers in polyethylene terephthalate products. Japanese Journal of Food Chemistry 10:138–144.

Mutsuga M, Tojima T, Kawamura Y, Tanamoto K. 2005. Survey of formaldehyde, acetaldehyde, and oligomers in polyethylene terephthalate food-packaging materials. Food Additives and Contaminants 22:783–789.

Nawrocki J, Dabrowska A, Borcz A. 2002. Investigation of carbonyl compounds in bottled waters from Poland. Water Research 36:4893–4901.

Nijssen B, Kamperman T, Jetten J. 1996. Acetaldehyde in mineral water stored in polyethylene terephthalate (PET) bottles: Odour threshold and quantification. Packaging Technology and Science 9:175–185.

Ramalho R, Cunha J, Teixeira P, Gibbs AP. 2001. Improved methods for the enumeration of heterotrophic bacteria in bottled mineral water. Journal of Microbiological Methods 44:97–103.

Sugaya N, Nakagawa T, Sakurai K, Morita M, Onodera S. 2001. Analysis of aldehydes in water by head space-GC/MS. Journal of Health Science 47:21–27.

Tsai GJ, Yu SC. 1997. Microbiological evaluation of bottled uncarbonated mineral water in Taiwan. International Journal of Food Microbiology 37:137–143.

Venkateswaran K, Hattori N, La Duc TM, Kern R. 2003. ATP as a biomarker of viable microorganisms in clean-room facilities. Journal of Microbiological Methods 52:367–377.

Villain F, Coudane J, Vert M. 1994. Thermal degradation of poly(ethylene terephthalate) and the estimation of volatile degradation products. Polymer Degradation and Stability 43:431–440.

Wyatt MD. 1983. Semi-automation of head space GC as applied to determination of acetaldehyde in polyethylene terephthalate beverage bottles. Journal of Chromatographic Science 21:508–511.

THE JOURNAL OF BIOLOGICAL CHEMISTRY VOL. 281, NO. 9, pp. 5484–5491, March 3, 2006

Structural Regions of MD-2 That Determine the Agonist-Antagonist Activity of Lipid IVa*

Received for publication, August 19, 2005, and in revised form, December 16, 2005 Published, JBC Papers in Press, December 31, 2005, DOI 10.1074/jbc.M509193200

Masashi Muroi and Ken-ichi Tanamoto[1]

From the Division of Microbiology, National Institute of Health Sciences, 1-18-1 Kamiyoga, Setagaya, Tokyo 158-8501, Japan

A cell surface receptor complex consisting of CD14, Toll-like receptor (TLR4), and MD-2 recognizes lipid A, the active moiety of lipopolysaccharide (LPS). *Escherichia coli*-type lipid A, a typical lipid A molecule, potently activates both human and mouse macrophage cells, whereas the lipid A precursor, lipid IVa, activates mouse macrophages but is inactive and acts as an LPS antagonist in human macrophages. This animal species-specific activity of lipid IVa involves the species differences in MD-2 structure. We explored the structural region of MD-2 that determines the agonistic and antagonistic activities of lipid IVa to induce nuclear factor-κB activation. By expressing human/mouse chimeric MD-2 together with mouse CD14 and TLR4 in human embryonic kidney 293 cells, we found that amino acid regions 57–79 and 108–135 of MD-2 determine the species-specific activity of lipid IVa. We also showed that the replacement of Thr^{57}, Val^{61}, and Glu^{122} of mouse MD-2 with corresponding human MD-2 sequence or alanines impaired the agonistic activity of lipid IVa, and antagonistic activity became evident. These mutations did not affect the activation of nuclear factor-κB, TLR4 oligomerization, and inducible phosphorylation of IκBα in response to *E. coli*-type lipid A. These results indicate that amino acid residues 57, 61, and 122 of mouse MD-2 are critical to determine the agonist-antagonist activity of lipid IVa and suggest that these amino acid residues may be involved in the discrimination of lipid A structure.

Bacterial lipopolysaccharide (LPS)[2] is a constituent of the outer membrane of the cell wall of Gram-negative bacteria and plays a major role in septic shock (1, 2). Engagement of LPS on the host cell results in rapid activation of a number of transcription factors, including NF-κB, which leads to production of inflammatory cytokines (3). Significant progress has been made in the identification of cell surface molecules that recognize LPS and transmit its signal to intracellular components. CD14, Toll-like receptor 4 (TLR4), and MD-2 participate in this molecular event and all of these molecules are necessary for cells to respond to picomolar concentrations of LPS (4, 5). A recent report (6) has suggested that sequential interactions of LPS with each of these molecules are required for optimal molecular recognition. LPS is first opsonized by the serum LPS-binding protein and then transferred to a CD14 molecule. This LPS-CD14 complex is further recognized by MD-2 to generate an LPS-MD-2 complex that produces TLR4-dependent cell stimulation. It has also been reported that MD-2 is necessary for TLR4 to undergo proper glycosylation and trafficking to the cell surface (7–9). Without MD-2, TLR4 is not able to reach the plasma membrane and resides predominantly in the Golgi apparatus. Thus, MD-2 is considered to play an important role for transferring LPS from CD14 to TLR4 and for correct cellular distribution of TLR4.

MD-2 also plays an important role for discriminating lipid A structure. The lipid A portion has been identified as the active center responsible for most LPS-induced biological effects (1, 10). *Escherichia coli*-type lipid A, a typical lipid A molecule, and its biosynthetic precursor lipid IVa have been synthesized chemically (compound 506 and 406, respectively), and their biological activities have been investigated extensively. Compound 506 and most varieties of LPS show little animal species-specific activity, whereas lipid IVa, as well as *Salmonella*-type lipid A, shows very little stimulatory activity and behaves as an antagonist in human macrophages, despite being potently active in murine macrophages (11, 12). This species-specific activity of lipid IVa and *Salmonella*-type lipid A has been attributed to the species difference in the structures of TLR4 (13, 14) and MD-2 (4, 15–17). Thus it is considered that MD-2 is also playing an important role for discriminating lipid A structure. To understand the molecular basis for this discriminating mechanism, we, in the present study, explored the structural region of MD-2 which determines the agonistic and antagonistic activities of lipid IVa.

EXPERIMENTAL PROCEDURES

Cell Culture and Reagents—The HEK293 cell line (obtained from the Human Science Research Resources Bank, Tokyo, Japan) was grown in Dulbecco's modified Eagle's medium (Invitrogen) supplemented with 10% (v/v) heat-inactivated fetal calf serum (Invitrogen), 100 units/ml penicillin, and 100 μg/ml streptomycin. Compound 506 and lipid IVa (compound 406) were obtained from Peptide Institute (Osaka, Japan). An antiserum against EIAV-tag epitope (amino acid sequence: ADRRIPGTAEE) was a kind gift from Dr. Nancy Rice (NCI-Frederick Cancer Research and Development Center). Stable transfectants expressing mouse CD14, EIAV-tagged mouse TLR4, FLAG-tagged mouse TLR4, and either EIAV-tagged mouse MD-2 or EIAV-tagged mouse MD-2-T57A,V61A,E122A were established as follows. After linearizing with PvuI, expression plasmids encoding the proteins described above were transfected into HEK293 cells by the calcium phosphate precipitation method. Stable transfectants were selected for G418 resistance at a concentration of 2 mg/ml. A monoclonal antibody (clone 5A5) that recognizes phosphorylated Ser^{32}-Ser^{36} of IκBα was purchased from Cell Signaling Technology (Danvers, MA).

Expression Plasmids—Expression plasmids encoding CD14, TLR4, and MD-2 as well as NF-κB-dependent luciferase reporter plasmid pELAM-L were described previously (16). Expression plasmids encoding MD-2 mutants were created by PCR-mediated mutagenesis, and mutations were confirmed by DNA sequencing.

NF-κB Reporter Assay—The NF-κB-dependent luciferase reporter assay was performed as described elsewhere (18). Briefly, HEK293 cells ($1–3 \times 10^5$/well) were plated in 12-well plates and on the following day

* This work was supported by a grant from the Ministry of the Environment. The costs of publication of this article were defrayed in part by the payment of page charges. This article must therefore be hereby marked "*advertisement*" in accordance with 18 U.S.C. Section 1734 solely to indicate this fact.

[1] To whom correspondence should be addressed. E-mail: tanamoto@nihs.go.jp.

[2] The abbreviations used are: LPS, lipopolysaccharide; HEK293, human embryonic kidney 293 cells; hMD-2, human MD-2; IκBα, inhibitor of NF-κB α; mMD-2, mouse MD-2; NF-κB, nuclear factor-κB; PBS, phosphate-buffered saline; TLR, Toll-like receptor.

transfected by the calcium phosphate precipitation method with 10 ng each of CD14, TLR4, and MD-2 mutant expression plasmids together with 0.1 μg of pELAM-L and 2.5 ng of phRL-TK (Promega, Madison, WI) for normalization. At 24 h after transfection, cells were stimulated for 6 h, and the reporter gene activity was measured according to the manufacturer's (Promega) instructions.

Detection of MD-2 Proteins Expressed on the Cell Surface—Detection of cell surface MD-2 was performed as described previously (19) with a slight modification. Briefly, HEK293 cells were plated in 6-cm dishes and transfected with indicated plasmids by the calcium phosphate precipitation method. After 24 h, the cells were transferred to 1.5-ml tubes and then washed twice with PBS. After suspension with 0.5 ml of PBS containing Ca^{2+} and Mg^{2+}, cells were exposed to 0.5 mg/ml of a membrane-impermeable biotinylation reagent (sulfo-NHS-LC-LC-biotin; Pierce) at 4 °C for 15 min. The reaction was quenched by adding 1 ml of culture medium, and then cell extracts were prepared with 0.35 ml of PBS containing 1% Nonidet P-40, 2 mM EDTA, and a protease inhibitor mix (Roche Applied Science). After centrifugation at 12,000 × *g* for 5 min, the supernatants obtained were incubated with immobilized streptavidin-agarose at 4 °C for 1 h. The agarose was washed three times with PBS containing 1% Nonidet P-40, 2 mM EDTA, and subsequently biotinylated proteins were eluted from the agarose by incubating with 5 mg/ml of a water-soluble biotin derivative (sulfo-NHS-biotin; Pierce) dissolved in a buffer (50 mM Tris, pH 8, 150 mM NaCl, 5 mM EDTA, 0.5% Nonidet P-40). The supernatant obtained was subjected to SDS-PAGE followed by Western blot analyzes.

Immunoprecipitation—HEK293 cells ($2–5 \times 10^7$ cells) stably expressing mouse CD14, EIAV-tagged mouse TLR4, FLAG-tagged mouse TLR4, and either EIAV-tagged mouse MD-2 or EIAV-tagged mouse MD-2-T57A,V61A,E122A were suspended into 1 ml of culture medium. After stimulation with compound 506 or lipid IVa, cells were washed with cold PBS, and cell extracts were prepared with PBS containing 0.5% Nonidet P-40, 1 μM okadaic acid, and a protease inhibitor mix (Roche Applied Science). To the cell extracts, anti-FLAG M2-agarose (Sigma) was added, and the mixture was incubated at 4 °C for 1 h. The agarose was washed three times with PBS containing 0.5% Nonidet P-40, and subsequently bound proteins were eluted from the agarose by incubating with an elution buffer (0.1 M glycine, pH 3.5, 0.5% Nonidet P-40). The supernatant obtained was subjected to SDS-PAGE followed by Western blot analyses.

RESULTS

Responsiveness to Lipid A Molecules in HEK293 Cells Expressing CD14, TLR4, and MD-2—We first attempted to confirm the involvement of MD-2 in the animal species-specific activity of lipid IVa in HEK293 cells, which only respond to lipid A for the activation of NF-κB when CD14, TLR4, and MD-2 molecules are present. In HEK293 cells transiently expressing mouse CD14, TLR4, and MD-2, both compound 506 and lipid IVa comparably stimulated the NF-κB-dependent reporter activity (Fig. 1*A*). When mouse MD-2 was replaced with human MD-2, compound 506 still actively stimulated cells, whereas the response to lipid IVa was substantially impaired (Fig. 1*B*).

To examine the antagonistic activity of lipid IVa, HEK293 cells expressing mouse CD14, TLR4, and either mouse MD-2 or human MD-2 were stimulated with compound 506 in the presence of increasing concentrations of lipid IVa (Fig. 2). In cells expressing mouse MD-2, NF-κB-dependent reporter activity stimulated with 10 ng/ml compound 506 was almost unaffected by lipid IVa. In contrast, when mouse MD-2 was replaced with human MD-2, lipid IVa inhibited the compound 506-induced activation of NF-κB in a concentration-dependent manner. These results indicate that the difference in MD-2 structure between human and mouse is involved in determining the agonist-antagonist activity of lipid IVa.

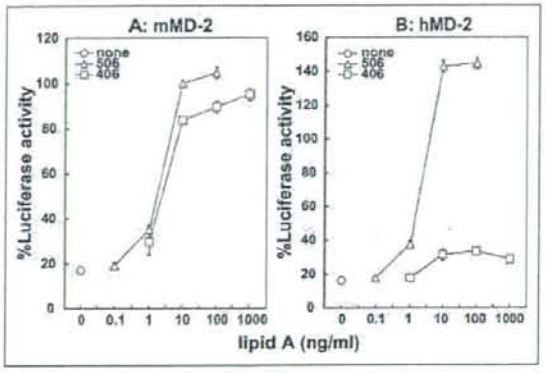

FIGURE 1. **Agonistic activities of lipid A and lipid IVa.** HEK293 cells were transiently transfected with mouse CD14, mouse TLR4, and either mouse MD-2 (*A*) or human MD-2 (*B*) expression plasmids together with an NF-κB-dependent luciferase reporter plasmid. After 24 h, cells were either unstimulated (○) or stimulated for 6 h with indicated concentrations of compound 506 (△) or lipid IVa (□), and luciferase activity was measured. The activity obtained with 10 ng/ml compound 506 in cells expressing mouse CD14, mouse TLR4, and mouse MD-2 was defined as 100%. Values are the means ± S.E. from seven independent experiments.

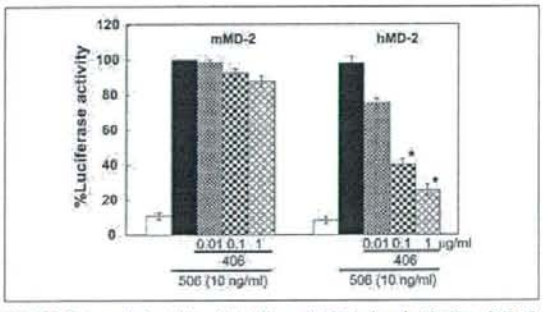

FIGURE 2. **Antagonistic activity of lipid IVa on lipid A-induced activation of NF-κB.** HEK293 cells were transiently transfected with mouse CD14, mouse TLR4, and either mouse MD-2 (*left five columns*) or human MD-2 (*right five columns*) expression plasmids together with an NF-κB-dependent luciferase reporter plasmid. After 24 h, cells were either unstimulated (*open columns*) or stimulated for 6 h with 10 ng/ml compound 506 (*506*) in the absence or presence of indicated concentrations of lipid IVa (*406*), and luciferase activity was measured. The activity obtained with 10 ng/ml compound 506 in cells expressing mouse CD14, mouse TLR4, and mouse MD-2 was defined as 100%. Values are the means ± S.E. from four independent experiments. * $p < 0.01$ (compared with the respective response in the absence of lipid IVa by two-tailed Student's *t* test).

MD-2 Structural Region Involved in Determining Agonist-Antagonist Activity of Lipid IVa—To explore the MD-2 structure required for the agonist-antagonist activity of lipid IVa, the coding region of mouse MD-2 was divided into six regions, and a series of MD-2 mutant plasmids in which each region was replaced with corresponding human MD-2 sequence was created (Fig. 3*A*). These chimeric mutants were expressed in HEK293 cells together with mouse CD14 and TLR4, and the NF-κB-dependent reporter activity was investigated (Fig. 3*B*). The cell surface expression of each of these MD-2 mutants was confirmed by Western blotting of biotinylated cell surface proteins, indicating that each of these mutants was similar enough to the parental mouse protein to be delivered to the cell membrane (Fig. 3*C*). Cells expressing each of the MD-2 mutants responded to compound 506 comparably with slight variations, indicating that all of these mutants functioned properly. In

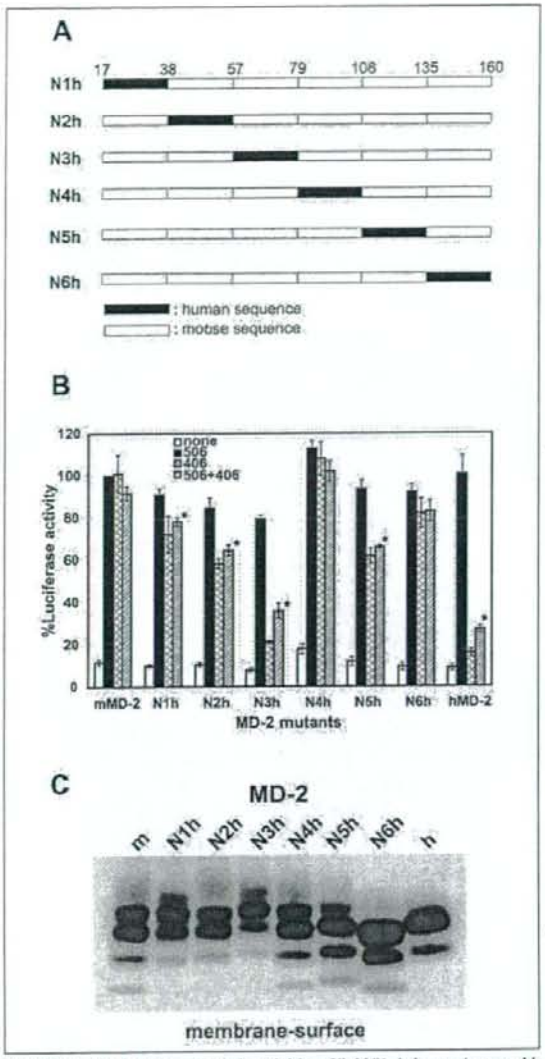

FIGURE 3. **Agonistic and antagonistic activities of lipid IVa in human/mouse chimeric MD-2.** *A*, schematic representation of human/mouse MD-2 constructs. The amino acid sequence of mouse MD-2 was divided into six regions at the indicated amino acid numbers, and each region was replaced with the corresponding human MD-2 sequence. The predicted signal peptide sequence (amino acids 1–16) was omitted. *B*, HEK293 cells were transiently transfected with mouse CD14, mouse TLR4, and the indicated mutant MD-2 expression plasmids together with an NF-κB-dependent luciferase reporter plasmid. After 24 h, cells were either unstimulated (*open columns*) or stimulated for 6 h with 10 ng/ml compound 506 (*506*), 1 μg/ml lipid IVa (*406*), or 10 ng/ml compound 506 in the presence of 1 μg/ml lipid IVa (*506 + 406*), and luciferase activity was measured. The activity obtained with 10 ng/ml compound 506 in cells expressing mouse CD14, mouse TLR4, and mouse MD-2 was defined as 100%. Values are the means ± S.E. from at least four independent experiments. * $p < 0.01$ (compared with the respective response in the absence of lipid IVa by two-tailed Student's *t* test). *C*, HEK293 cells were transiently transfected with mouse CD14, mouse TLR4, and the indicated mutant MD-2 expression plasmids. After 24 h, cell surface proteins were biotinylated with a membrane-impermeable biotinylation reagent, and biotinylated proteins from cell extracts were collected with streptavidin-agarose. After washing, biotinylated proteins were eluted from the agarose by incubating with a water-soluble biotin derivative, and the supernatant obtained was subjected to SDS-PAGE followed by Western blot analysis to detect membrane surface MD-2 mutant proteins. Similar results were obtained in two additional experiments.

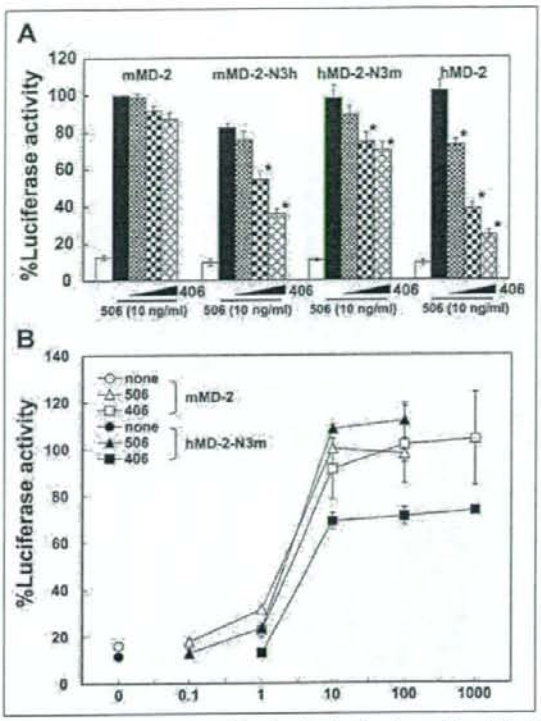

FIGURE 4. **N3 region of MD-2 is partly involved in animal species-specific activity of lipid IVa.** HEK293 cells were transiently transfected with mouse CD14, mouse TLR4, and the indicated mutant MD-2 expression plasmids together with an NF-κB-dependent luciferase reporter plasmid. After 24 h, cells were either unstimulated (*open columns*) or stimulated for 6 h with 10 ng/ml compound 506 (*506*) in the absence or presence of increasing concentrations (0.01, 0.1, and 1 μg/ml) of lipid IVa (*406*) in *A*, or were either unstimulated (○, ●) or stimulated for 6 h with the indicated concentrations of compound 506 (△, ▲) or lipid IVa (□, ■) in *B*, and luciferase activity was measured. The activity obtained with 10 ng/ml compound 506 in cells expressing mouse CD14, mouse TLR4, and mouse MD-2 was defined as 100%, and luciferase activity was measured. The activity obtained with 10 ng/ml compound 506 in cells expressing mouse CD14, mouse TLR4, and mouse MD-2 was defined as 100%. Values are the means ± S.E. from at least three independent experiments. * $p < 0.01$ (compared with the respective response in the absence of lipid IVa by two-tailed Student's *t* test).

contrast, the activity of lipid IVa varied and was substantially impaired in cells expressing the mMD-2-N3h mutant. The activity was similar to that observed in cells expressing human MD-2. A partial reduction with a statistical significance in the activity of lipid IVa was also observed in mMD-2-N2h and mMD-2-N5h mutants as well as in mMD-2-N1h to a lesser extent. The antagonistic activity of lipid IVa was also studied in these MD-2 mutants by stimulating with compound 506 in the presence of lipid IVa. (Fig. 3*B*). In cells expressing mouse MD-2, lipid IVa did not inhibit the compound 506-induced activation of NF-κB, whereas in cells expressing human MD-2 the activity of compound 506 was inhibited substantially by lipid IVa as mentioned above. When MD-2 mutants were expressed, the activity of compound 506 was inhibited by lipid IVa in cells expressing the mMD-2-N3h mutant to a degree similar to that observed with human MD-2. These results suggest that the N3 region of MD-2 is involved in the animal species-specific activity of lipid IVa.

We next asked whether the N3 region of MD-2 is critical for establishing the agonist-antagonist activity of lipid IVa. To address this, HEK293 cells expressing mouse CD14, TLR4, and N3 chimeras or

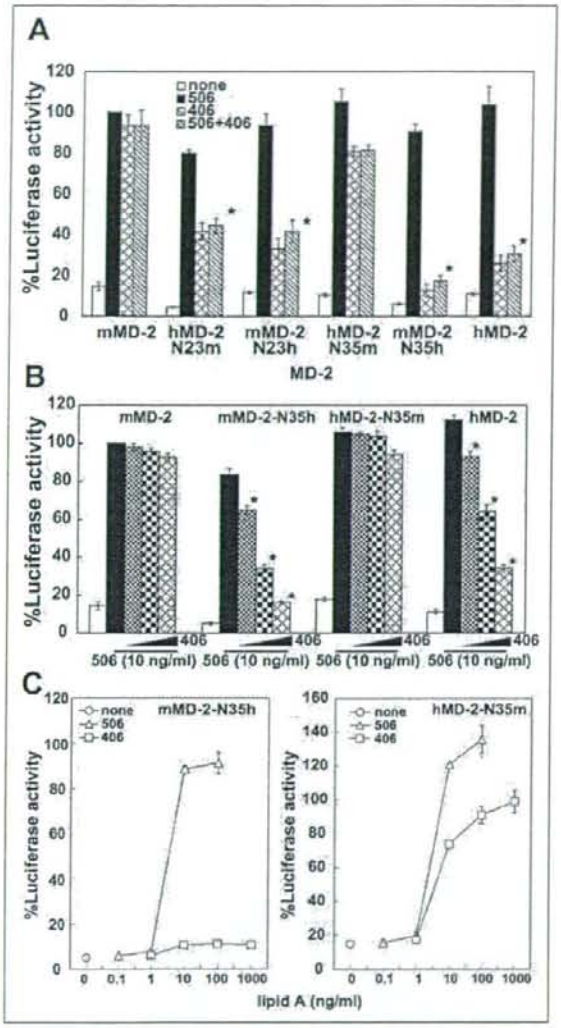

FIGURE 5. **N3 and N5 regions of MD-2 are responsible for animal species-specific activity of lipid IVa.** HEK293 cells were transiently transfected with mouse CD14, mouse TLR4, and the indicated mutant MD-2 expression plasmids together with an NF-κB-dependent luciferase reporter plasmid. After 24 h, cells were either unstimulated (*open columns*) or stimulated for 6 h with 10 ng/ml compound 506 (*506*), 1 μg/ml lipid IVa (*406*), or 10 ng/ml compound 506 in the presence of 1 μg/ml of lipid IVa (*506 + 406*) in *A*, or were either unstimulated (*open columns*) or stimulated for 6 h with 10 ng/ml compound 506 in the absence or presence of increasing concentrations (0.01, 0.1, and 1 μg/ml) of lipid IVa in *B*, or were either unstimulated (○) or stimulated for 6 h with the indicated concentrations of compound 506 (△) or lipid IVa (□) in *C*, and luciferase activity was measured. The activity obtained with 10 ng/ml compound 506 in cells expressing mouse CD14, mouse TLR4, and mouse MD-2 was defined as 100%. Values are the means ± S.E. from at least three independent experiments. * $p < 0.01$ (compared with the respective response in the absence of lipid IVa by two-tailed Student's *t* test).

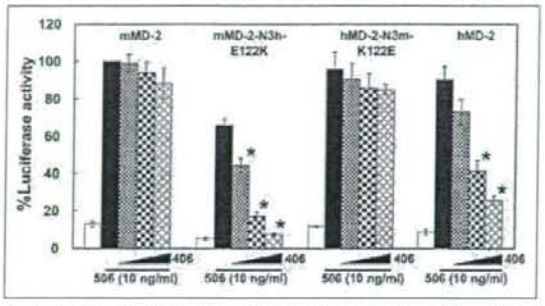

FIGURE 6. **Amino acid 122 of MD-2 is involved in animal species-specific activity of lipid IVa.** HEK293 cells were transiently transfected with mouse CD14, mouse TLR4, and the indicated mutant MD-2 expression plasmids together with an NF-κB-dependent luciferase reporter plasmid. After 24 h, cells were either unstimulated (*open columns*) or stimulated for 6 h with 10 ng/ml compound 506 (*506*) in the absence or presence of increasing concentrations (0.01, 0.1, and 1 μg/ml) of lipid IVa (*406*), and luciferase activity was measured. The activity obtained with 10 ng/ml compound 506 in cells expressing mouse CD14, mouse TLR4, and mouse MD-2 was defined as 100%. Values are the means ± S.E. from at least three independent experiments. * $p < 0.01$ (compared with the respective response in the absence of lipid IVa by two-tailed Student's *t* test).

parental MD-2 were stimulated with compound 506 in the presence of increasing concentrations of lipid IVa (Fig. 4*A*). As expected, lipid IVa concentration-dependently inhibited the compound 506-induced activation of NF-κB in cells expressing the N3h mutant; however, the inhibitory activity was relatively weaker than that observed in cells expressing the parental hMD-2. If the N3 region of MD-2 is the only region responsible for the species-specific activity of lipid IVa, it was expected that replacing the N3 region of human MD-2 with the corresponding mouse MD-2 sequence would show the mouse phenotype. However, a slight inhibitory effect of lipid IVa was still observed in cells expressing the N3m chimera (hMD-2-N3m). In addition, the agonistic activity of lipid IVa in cells expressing this N3m chimera only reached ~73% of the activity observed in cells expressing the parental mouse MD-2 (Fig. 4*B*).

The above result brought us to explore another MD-2 region, in addition to the N3 region, that is involved in the agonist-antagonist activity of lipid IVa. Because a slight antagonistic activity of lipid IVa was observed in mMD-2-N2h and mMD-2-N5h mutants (Fig. 3*B*), we created MD-2 mutant plasmids in which both the N2 and N3 regions or the N3 and N5 regions were mutated. These MD-2 mutants were used to examine the NF-κB-dependent reporter activity in HEK293 cells expressing mouse CD14, TLR4 (Fig. 5*A*). Compound 506 showed activity comparable with all of these MD-2 mutants. With the MD-2 mutant in which the N2 and N3 regions of human MD-2 were replaced with corresponding mouse sequences (hMD-2-N23m) and the mutant in which the N2 and N3 regions of mouse MD-2 were replaced with corresponding human sequences (mMD-2-N23h), lipid IVa showed partial agonistic and partial antagonistic activities. Contrarily, lipid IVa showed a strong agonistic activity with the MD-2 mutant in which the N3 and N5 regions of human MD-2 were replaced with corresponding mouse sequences (hMD-2-N35m), and almost no agonistic activity of lipid IVa, even at 1 μg/ml, was observed with a mutant in which the N3 and N5 regions of mouse MD-2 were replaced with corresponding human sequences (mMD-2-N35h). The antagonistic activity of lipid IVa was also examined with these mutants (Fig. 5*B*). Almost no antagonistic activity was observed with hMD-2-N35m, and a clear antagonistic activity was observed with mMD-2-N35h. In addition, lipid IVa caused almost no agonistic activity in cells expressing mMD-2-N35h and showed a potent agonistic activity comparable with that observed with wild-type mouse MD-2 (see Fig. 1*A*) in cells expressing hMD-2-N35m (Fig. 5*C*). These results indicate that both of the N3 and N5 regions of MD-2 are involved in determining the agonist-antagonist activity of lipid IVa.

MD-2 Structural Region Involved in Antagonistic Activity of Lipid IVa—Replacement of the N3 and N5 regions of mouse MD-2 with corresponding human sequences changed the activity of lipid IVa from agonistic to antagonistic without affecting the activity of compound

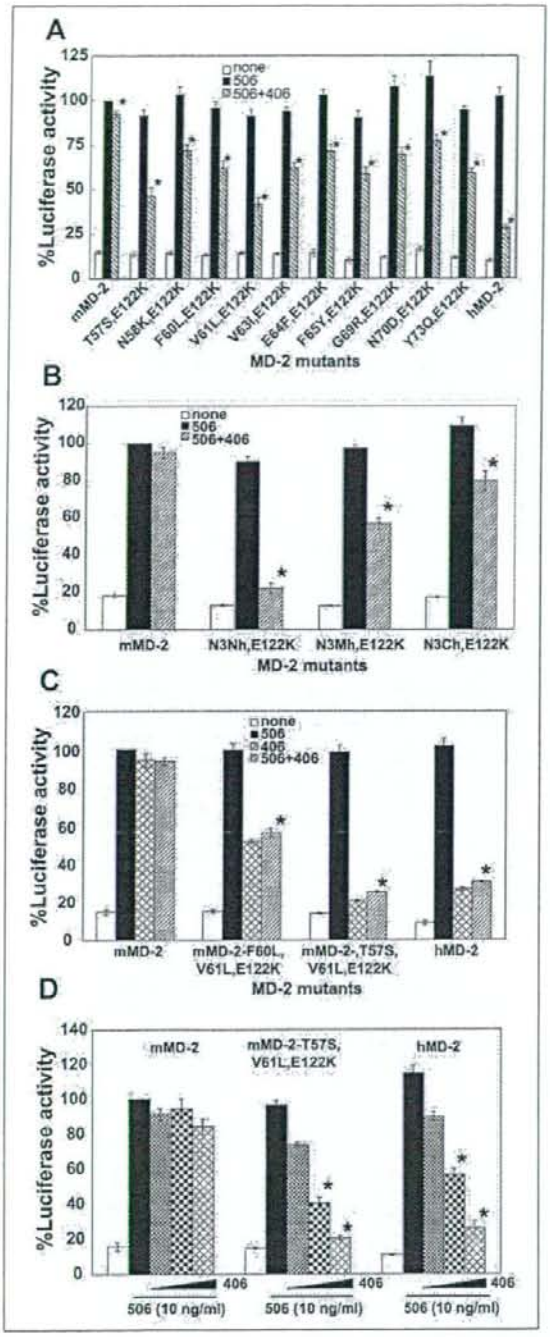

FIGURE 7. **Amino acid residues 57, 61, and 122 of MD-2 are involved in animal species-specific activity of lipid IVa.** HEK293 cells were transiently transfected with mouse CD14, mouse TLR4, and the indicated mutant MD-2 expression plasmids together with an NF-κB-dependent luciferase reporter plasmid. After 24 h, cells were either unstimulated (*open columns*) or stimulated for 6 h with 10 ng/ml compound 506 (*506*) or 10 ng/ml compound 506 in the presence of lipid IVa (*506 + 406*) in *A* and *B*, were either unstimulated (*open columns*) or stimulated for 6 h with 10 ng/ml compound 506, 1 μg/ml lipid IVa, or 10 ng/ml compound 506 in the presence of 1 μg/ml lipid IVa in *C*, or were either unstimulated (*open columns*) or stimulated for 6 h with 10 ng/ml compound 506 in the absence or presence of increasing concentrations (0.01, 0.1, and 1 μg/ml) of lipid IVa in *D*, and luciferase activity was measured. The activity obtained with 10 ng/ml compound 506 in cells expressing mouse CD14, mouse TLR4, and mouse MD-2 was defined as 100%. Values are the means ± S.E. from at least three independent experiments. * $p < 0.01$ (compared with the respective response in the absence of lipid IVa by two-tailed Student's *t* test).

506. Human and mouse MD-2 possess a similar amino acid sequence in their N5 regions with only a major difference at amino acid 122, a change in charge. Thus, to investigate the involvement of amino acid 122 of MD-2 in the activity of lipid IVa, we examined the antagonistic activity of lipid IVa with a mouse MD-2 mutant (mMD-2-N3h-E122K) in which the N3 region and amino acid 122 were replaced with the corresponding human sequence and a human MD-2 mutant (hMD-2-N3m-K122E) in which the N3 region and amino acid 122 were replaced with the corresponding mouse sequence (Fig. 6). A stronger antagonistic activity was observed in cells expressing mMD-2-N3h-E122K compared with those expressing mMD-2-N3h (see Fig. 4). On the other hand, almost no antagonistic effect was observed with hMD-2-N3m-K122E. It is therefore likely that the involvement of the N5 region is explained by amino acid 122.

We next asked whether the involvement of the N3 region was also explained at the amino acid level. To address this, each amino acid of the N3 region of mouse MD-2, carrying E122K mutation, was replaced individually with the corresponding human amino acid residue, and the antagonistic activity of lipid IVa was examined (Fig. 7*A*). Although compound 506-induced activation of NF-κB was inhibited to some extent in cells expressing these MD-2 mutants, sufficient antagonistic activities were not observed. Thus we created mouse MD-2 mutant plasmids in which the overlapping three regions (amino acid residues 57–65, 64–73, and 69–78) within N3 and amino acid 122 were replaced with the corresponding human sequences (each named as N3Nh,E122K, N3Mh,E122K, N3Ch,E122K), and the antagonistic activity of lipid IVa was examined (Fig. 7*B*). A potent antagonistic effect of lipid IVa was observed with the N3Nh,E122K mutant, indicating that amino acid residues 57–65 and 122 of human MD-2 play a role in the antagonistic effect. Because the N3 region of human MD-2 is leucine-rich, we suspected that two leucines (amino acids 60 and 61) might be involved in the antagonistic effect. Thus we created a mouse MD-2 mutant plasmid carrying F60L, V61L, and E122K mutations. Furthermore, because relatively potent antagonistic effects were observed with T57S,E122K and V61L,E122 mutants (Fig. 7*A*), we also created a mouse MD-2 mutant plasmid carrying T57S, V61L, and E122K mutations. Agonistic effects of compound 506 and lipid IVa as well as antagonistic effects of lipid IVa were examined (Fig. 7*C*). Only partial agonistic and antagonistic activities of lipid IVa were observed with the mMD-2-F60L,V61L,E122K mutant. However, these activities and the concentration-inhibition effect of lipid IVa (Fig. 7*D*) in cells expressing the mMD-2-T57S,V61L,E122K mutant were comparable with those observed in hMD-2, indicating a critical role of these three amino acid residues (Ser^{57}, Leu^{61}, and Lys^{122}) for expressing the antagonistic activity.

MD-2 Structural Region Involved in Agonistic Activity of Lipid IVa—Mutation of Thr^{57}, Val^{61}, and Glu^{122} of mouse MD-2 into corresponding human MD-2 sequences caused not only the appearance of antagonistic activity of lipid IVa but also the disappearance of its agonistic activity, without losing the agonistic activity of compound 506 (Fig. 7*C*). Thus we next asked whether these three amino acid residues

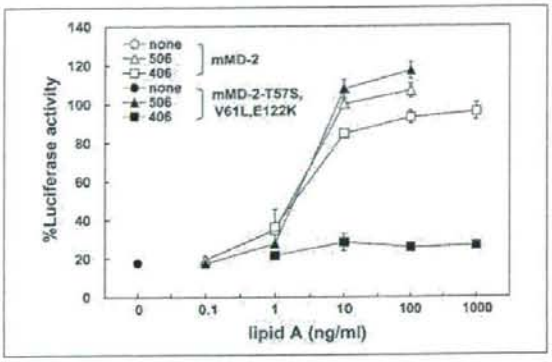

FIGURE 8. **Replacement of Thr^{57}, Val^{61}, and Glu^{122} of mouse MD-2 with corresponding human MD-2 sequence loses the agonistic activity of lipid IVa without affecting lipid A activity.** HEK293 cells were transiently transfected with mouse CD14, mouse TLR4, and the indicated MD-2 expression plasmids together with an NF-κB-dependent luciferase reporter plasmid. After 24 h, cells were either unstimulated (○, ●) or stimulated for 6 h with indicated concentrations of compound 506 (△, ▲) or lipid IVa (□, ■), and luciferase activity was measured. The activity obtained with 10 ng/ml compound 506 in cells expressing mouse CD14, mouse TLR4, and mouse MD-2 was defined as 100%. Values are the means ± S.E. from four independent experiments.

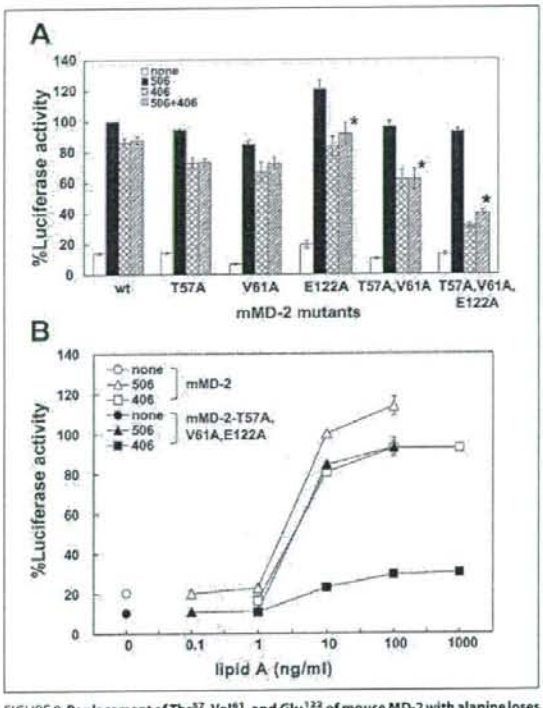

FIGURE 9. **Replacement of Thr^{57}, Val^{61}, and Glu^{122} of mouse MD-2 with alanine loses the agonistic activity of lipid IVa without affecting lipid A activity.** HEK293 cells were transiently transfected with mouse CD14, mouse TLR4, and the indicated MD-2 expression plasmids together with an NF-κB-dependent luciferase reporter plasmid. After 24 h, cells were either unstimulated (*open columns*) or stimulated for 6 h with 10 ng/ml compound 506 (*506*), 1 μg/ml lipid IVa (*406*), or 10 ng/ml compound 506 in the presence of 1 μg/ml lipid IVa (*506 + 406*) in *A*, or were either unstimulated (○, ●) or stimulated for 6 h with the indicated concentrations of compound 506 (△, ▲) or lipid IVa (□, ■) in *B*, and luciferase activity was measured. The activity obtained with 10 ng/ml compound 506 in cells expressing mouse CD14, mouse TLR4, and mouse MD-2 was defined as 100%. Values are the means ± S.E. from three independent experiments. * $p < 0.01$ (compared with the respective response in the absence of lipid IVa by two-tailed Student's *t* test). *wt*, wild-type.

of mouse MD-2 were selectively involved in the agonistic activity of lipid IVa. To address this, we examined the agonistic activities of lipid IVa and compound 506 in cells expressing mMD-2-T57S,V61L,E122K together with mouse CD14 and TLR4 (Fig. 8). In these cells, compound 506 induced potent activation of NF-κB comparable with that observed in cells expressing wild-type mouse MD-2, whereas almost no agonistic activity was observed with lipid IVa at concentrations from 1 to 1,000 ng/ml. Although the mutation of glutamic acid to a lysine caused a charge reversal, mutations from threonine to serine and from valine to leucine may not cause significant changes. It is, therefore, still possible that compound 506 may require these amino acid residues for its agonistic activity, but these changes in amino acid residues may be tolerated. To address this, we mutated these three amino acid residues in mouse MD-2 into alanines either individually or in combinations and examined the agonistic activities of compound 506 and lipid IVa as well as the antagonistic activity of lipid IVa (Fig. 9). Although the agonistic activity of compound 506 with the E122A mutation was slightly enhanced, none of the mutations caused significant changes in the activity of compound 506. No significant changes in the agonistic and antagonistic activities of lipid IVa were observed with each point mutant or the T57S,V61A mutant, whereas the concurrent mutation of all three amino acid residues substantially decreased the agonistic activity, and the antagonistic activity was also evident (Fig. 9*A*). The concentration-response effects showed that the activity of compound 506 was decreased only slightly by the concurrent mutation of all three amino acid residues, whereas the activity of lipid IVa was substantially impaired (Fig. 9*B*). These results indicate that these three amino acid residues are selectively involved in the agonistic activity of lipid IVa and critical for determining its agonist-antagonist activity.

Role of Thr^{57}, Val^{61}, and Glu^{122} of MD-2 in TLR4 Signaling—The role of Thr^{57}, Val^{61}, and Glu^{122} of mouse MD-2 in TLR4 signaling was studied in HEK293 cells stably expressing mouse CD14, EIAV-tagged mouse TLR4, FLAG-tagged mouse TLR4, and either EIAV-tagged mouse MD-2 or EIAV-tagged mouse MD-2-T57A,V61A,E122A. These cells were stimulated with compound 506 or lipid IVa, and TLR4 oligomerization was examined (Fig. 10). For this, FLAG-tagged TLR4 was immunoprecipitated, and coprecipitation of EIAV-tagged TLR4 was detected by Western blotting. Coprecipitations of EIAV-tagged TLR4 were barely detectable without stimulations but were detectable after compound 506 stimulation in both stable transfectants. After lipid IVa stimulation, the coprecipitation was also detected in cells expressing wild-

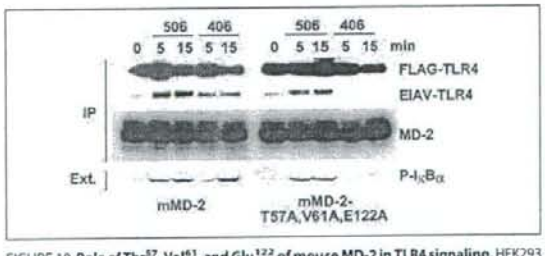

FIGURE 10. **Role of Thr^{57}, Val^{61}, and Glu^{122} of mouse MD-2 in TLR4 signaling.** HEK293 cells stably expressing mouse CD14, EIAV-tagged mouse TLR4, FLAG-tagged mouse TLR4, and either EIAV-tagged mouse MD-2 (*left five lanes*) or EIAV-tagged mouse MD-2-T57A,V61A,E122A (*right five lanes*) were stimulated with 100 ng/ml compound 506 or 1 μg/ml lipid IVa for the indicated times. Then, cell extracts (*Ext.*) were prepared, and FLAG-tagged TLR4 was immunoprecipitated (*IP*). Precipitated FLAG-tagged TLR4 and coprecipitated EIAV-tagged TLR4 as well as MD-2 proteins were detected by Western blotting. A part of cell extracts prepared above were subjected to the detection of IκBα protein phosphorylated at Ser^{32}-Ser^{36} (*P-IκBα*) by Western blotting. Similar results were obtained in two additional experiments.

type MD-2 but was barely detectable in cells expressing mMD-2-T57A,V61A,E122A. Both the wild-type and mutant MD-2 were coprecipitated with TLR4 without ligand stimulation, and the amount coprecipitated was unaffected by stimulations. In parallel with TLR4 oligomerization, the inducible phosphorylation of IκBα was observed in response to compound 506 in both stable transfectants. The phosphorylation was also observed in response to lipid IVa in cells expressing wild-type MD-2 but was barely detectable in cells expressing mMD-2-T57A,V61A,E122A. These results support the above conclusion that Thr^{57}, Val^{61}, and Glu^{122} of mouse MD-2 are selectively involved in the agonistic activity of lipid IVa and critical for determining its agonist-antagonist activity.

DISCUSSION

In the present study, we investigated the structural region of MD-2 required for agonistic and antagonistic activities of lipid IVa by utilizing its animal species-specific activity. The involvement of MD-2 in animal species-specific activity of lipid IVa has been demonstrated previously by expressing human and mouse MD-2 in human monocytic THP-1 cells (4), mouse pro B Ba/F3 cells (15), and HEK293 cells (17). In the present study, we confirmed that the lipid IVa-induced activation of NF-κB in HEK293 cells expressing mouse CD14, TLR4, and MD-2 was substantially impaired when mouse MD-2 was replaced with human MD-2. The activity of compound 506, a typical lipid A molecule, was not significantly affected by the replacement, indicating that both human and mouse MD-2 are functional on mouse TLR4. Thus, in the present study, we created mouse/human chimeric MD-2 mutant plasmids and found that both the N3 (amino acids 57–79) and N5 (amino acids 108–135) regions of MD-2 were involved in the species-specific activity of lipid IVa. We further narrowed the region down and found that the concurrent replacement of Thr^{57}, Val^{61}, and Glu^{122} of mouse MD-2 with the corresponding human MD-2 amino acids substantially decreased the agonistic activity of lipid IVa without affecting the activity of compound 506. The replacement of each of these amino acid residues individually or as pairs was not enough to lose the activity, indicating that these three residues together contribute to the species-specific activity of lipid IVa. A tertiary structure model of human MD-2, reported by Gruber *et al.* (20), shows that amino acid residues 57, 61, and 122 of MD-2 are sterically located in close proximity. Thus the domain created by these three amino acid residues may be involved in determining the agonist-antagonist activity of lipid IVa.

The mutation of Thr^{57} to Ser, Val^{61} to Leu, and Glu^{122} to Lys of mouse MD-2 substantially decreased the agonistic activity of lipid IVa, whereas these replacements did not affect the activity of compound 506. Because the difference in amino acid structure between Thr and Ser or between Val and Leu is only one methyl or methylene moiety, there was still the possibility that these changes in amino acid residues may be tolerated even though compound 506 may require these amino acid residues for full agonistic activity. Thus we examined the activity of compound 506 in a mouse MD-2 mutant in which Thr^{57}, Val^{61}, and Glu^{122} were replaced with alanines, and we found that the activity was not affected by these substitutions, whereas the activity of lipid IVa was substantially impaired. It is therefore likely that these three amino acid residues are selectively involved in the agonistic activity of lipid IVa.

The replacement of amino acid residues 57, 61, and 122 of mouse MD-2 with corresponding human MD-2 amino acids substantially decreased the agonistic activity of lipid IVa. However, replacement of amino acid residues 57, 61, and 122 of human MD-2 with the corresponding mouse MD-2 amino acid residues restored the agonistic activity of lipid IVa only to ~50% of the activity observed in mouse MD-2 (data not shown). Replacement of the N3 region, and replacement of amino acid 122 in addition to the N3 region of human MD-2 with corresponding mouse MD-2 sequence restored the activity to ~73% (Fig. 4*B*) and 90% (data not shown), respectively. Therefore, these three amino acid residues are necessary for the agonistic activity of lipid IVa, but additional amino acid residues in the N3 region may be required for its full agonistic activity.

It has been reported, in studies using soluble MD-2 (6, 21–23) and a peptide fragment of MD-2 (24) that LPS directly binds to MD-2 in a highly basic region (amino acids 119–132). In our study, the mutation of Thr^{57}, Val^{61}, and Glu^{122} of mouse MD-2 to alanines (Fig. 9) or the mutation of Ser^{57}, Leu^{61}, and Lys^{122} of human MD-2 to corresponding mouse MD-2 amino acid residues (data not shown) did not affect the agonistic activity of compound 506, indicating that these three amino acid residues are not involved in lipid A binding. In addition, it is unlikely that these three amino acid residues are involved in lipid IVa binding because lipid IVa showed an antagonistic effect in cells expressing the mouse MD-2 mutant in which all three of these amino acid residues were replaced with the corresponding human MD-2 amino acid residues or with alanines. For TLR4 signaling, the interaction between MD-2 and TLR4 (7, 22, 23, 25), as well as dimerization of TLR4 (26, 27) were reported to be important. For the interaction with TLR4, Cys^{95}, Tyr^{102}, and Cys^{105} of human MD-2 have been reported to be involved (22–23, 25). Miyake (5) and Gangloff and Gay (28) have proposed that MD-2 plays an important role in regulating TLR4 dimerization upon LPS binding. Because the ability of MD-2 to associate with TLR4 and compound 506-induced TLR4 dimerization as well as inducible phosphorylation of IκBα were not affected by the mutation of Thr^{57}, Val^{61}, and Glu^{122} of mouse MD-2 (Fig. 10), these amino acid residues are unlikely to be involved in interactions with TLR4 or in TLR4 dimerization. These amino acid residues may participate in the discrimination of lipid A structure.

Acknowledgments—We thank Keisuke Nakada and Takamasa Hiratsuka for technical assistance.

REFERENCES

1. Schletter, J., Heine, H., Ulmer, A. J., and Rietschel, E. T. (1995) *Arch. Microbiol.* **164,** 383–389
2. Ulevitch, R. J., and Tobias, P. S. (1995) *Annu. Rev. Immunol.* **13,** 437–457
3. Hatada, E. N., Krappmann, D., and Scheidereit, C. (2000) *Curr. Opin. Immunol.* **12,** 52–58
4. Fujihara, M., Muroi, M., Tanamoto, K., Suzuki, T., Azuma, H., and Ikeda, H. (2003) *Pharmacol. Ther.* **100,** 171–194
5. Miyake, K. (2004) *Trends Microbiol.* **12,** 186–192
6. Gioannini, T. L., Teghanemt, A., Zhang, D., Coussens, N. P., Dockstader, W., Ramaswamy, S., and Weiss, J. P. (2004) *Proc. Natl. Acad. Sci. U. S. A.* **101,** 4186–4191
7. Nagai, Y., Akashi, S., Nagafuku, M., Ogata, M., Iwakura, Y., Akira, S., Kitamura, T., Kosugi, A., Kimoto, M., and Miyake, K. (2002) *Nat. Immunol.* **3,** 667–672
8. da Silva, C. J., and Ulevitch, R. J. (2002) *J. Biol. Chem.* **277,** 1845–1854
9. Ohnishi, T., Muroi, M., and Tanamoto, K. (2003) *Clin. Diagn. Lab. Immunol.* **10,** 405–410
10. Lüderitz, O., Freudenberg, M., Galanos, C., Lehmann, E. T., Rietschel, E. T., and Shaw, D. H. (1982) *Curr. Top Membr. Transp.* **17,** 79–151
11. Tanamoto, K., and Azumi, S. (2000) *J. Immunol.* **164,** 3149–3156
12. Means, T. K., Golenbock, D. T., and Fenton, M. J. (2000) *Cytokine Growth Factor Rev.* **11,** 219–232
13. Poltorak, A., Ricciardi-Castagnoli, P., Citterio, S., and Beutler, B. (2000) *Proc. Natl. Acad. Sci. U. S. A.* **97,** 2163–2167
14. Lien, E., Means, T. K., Heine, H., Yoshimura, A., Kusumoto, S., Fukase, K., Fenton, M. J., Oikawa, M., Qureshi, N., Monks, B., Finberg, R. W., Ingalls, R. R., and Golenbock, D. T. (2000) *J. Clin. Invest.* **105,** 497–504
15. Akashi, S., Nagai, Y., Ogata, H., Oikawa, M., Fukase, K., Kusumoto, S., Kawasaki, K., Nishijima, M., Hayashi, S., Kimoto, M., and Miyake, K. (2001) *Int. Immunol.* **13,**

1595–1599
16. Muroi, M., Ohnishi, T., and Tanamoto, K. (2002) *Infect. Immun.* **70**, 3546–3550
17. Hajjar, A. M., Ernst, R. K., Tsai, J. H., Wilson, C. B., and Miller, S. I. (2002) *Nat. Immunol.* **3**, 354–359
18. Muroi, M., and Tanamoto, K. (2002) *Infect. Immun.* **70**, 6043–6047
19. Muroi, M., Ohnishi, T., and Tanamoto, K. (2002) *J. Biol. Chem.* **277**, 42372–42379
20. Gruber, A., Manček, M., Wagner, H., Kirschning, C. J., and Jerala, R. (2004) *J. Biol. Chem.* **279**, 28475–28482
21. Viriyakosol, S., Tobias, P. S., Kitchens, R. L., and Kirkland, T. N. (2001) *J. Biol. Chem.* **276**, 38044–38051
22. Visintin, A., Latz, E., Monks, B. G., Espevik, T., and Golenbock, D. T. (2003) *J. Biol. Chem.* **278**, 48313–48320
23. Re, F., and Strominger, J. L. (2003) *J. Immunol.* **171**, 5272–5276
24. Manček, M., Pristovšek, P., and Jerala, R. (2002) *Biochem. Biophys. Res. Commun.* **292**, 880–885
25. Kawasaki, K., Nogawa, H., and Nishijima, M. (2003) *J. Immunol.* **170**, 413–420
26. Medzhitov, R., Preston-Hurlburt, P., and Janeway, C. A. J. (1997) *Nature* **388**, 394–397
27. Zhang, H., Tay, P. N., Cao, W., Li, W., and Lu, J. (2002) *FEBS Lett.* **532**, 171–176
28. Gangloff, M., and Gay, N. J. (2004) *Trends Biochem. Sci.* **29**, 294–300

SHORT COMMUNICATION

Effects of possible endocrine disruptors on MyD88-independent TLR4 signaling

Takahiro Ohnishi, Tomohisa Yoshida, Arisa Igarashi, Masashi Muroi & Ken-ichi Tanamoto

Division of Microbiology, National Institute of Health Sciences, Setagaya, Tokyo, Japan

Correspondence: Ken-ichi Tanamoto, Division of Microbiology, National Institute of Health Sciences, 1-18-1 Kamiyoga, Setagaya, Tokyo 158-8501, Japan. Tel.: +81 3 3700 1141, ext. 321; fax: +81 3 3700 9484; e-mail: tanamoto@nihs.go.jp

Received 3 July 2007; revised 13 September 2007; accepted 8 October 2007.
First published online 20 December 2007.

DOI:10.1111/j.1574-695X.2007.00355.x

Editor: Patrick Brennan

Keywords
endocrine disruptors; IFN-β; lipopolysaccharide; bacterial lipoprotein; macrophage.

Abstract

Endocrine disrupting chemicals (EDCs) may potentially worsen infectious diseases because EDCs disturb human immune function by interfering with endocrine balance. To evaluate the influence of EDCs on the innate immune function of macrophages, we investigated the effects of 37 possible EDCs on lipopolysaccharide-induced activation of the IFN-β promoter. Alachlor, atrazine, benomyl, bisphenol A, carbaryl, diethyl phthalate, dipropyl phthalate, kelthane, kepone, malathion, methoxychlor, octachlorostyrene, pentachlorophenol, nonyl phenol, *p*-octylphenol, simazine and ziram all inhibited the activation. Kepone and ziram showed strong inhibitory effects. Aldicarb, amitrole, benzophenone, butyl benzyl phthalate, 2,4-dichlorophenoxy acetic acid, dibutyl phthalate, 2,4-dichlorophenol, dicyclohexyl phthalate, diethylhexyl adipate, diethylhexyl phthalate, dihexyl phthalate, di-*n*-pentyl phthalate, methomyl, metribuzin, nitrofen, 4-nitrotoluene, permethrin, trifluralin, 2,4,5-trichlorophenoxyacetic acid and vinclozolin had no significant effects at 100 μM. These results indicate that some agrochemicals and resin-related chemicals may potentially inhibit macrophage function, which suggests that endocrine disruptors may influence the development of infectious diseases.

Endocrine disrupting chemicals (EDCs) are exogenous substances that mimic, antagonize, impair, enhance or inhibit the actions of endogenous hormones and in turn cause abnormalities of growth, reproduction, development, behavior and immune function, or cause malignant tumors (Safe *et al.*, 1998; Schrenk, 1998; Eskenazi *et al.*, 2000). EDCs exert their activity at multiple sites by multiple mechanisms. Receptor-mediated mechanisms have been well studied, but other mechanisms including effects on hormone synthesis, transport and metabolism are also involved (Masuyama *et al.*, 2000; Inoshita *et al.*, 2003). However, the secondary effects of EDCs, such as the influence on infectious diseases, are not well known. Infectious diseases are caused by microbial invasion. The human body is equipped with a complicated immune system to cope with microbial invasion. Disorder of this well-organized immune system may lead to the development of serious infectious diseases; therefore, it is possible that EDCs may worsen the effects of infectious diseases because any disorder of the endocrine system seriously disturbs immune function. Macrophages are recognized as an important component of the host immune system, and are activated by microbial components, especially by lipopolysaccharide (Fujihara *et al.*, 2003). Previously, we investigated the effects of various possible EDCs on macrophage activation and found that some EDCs strongly inhibit lipopolysaccharide-induced TNF-α and nitric oxide production by macrophages (Hong *et al.*, 2004). Since the activation of the transcription factor nuclear factor (NF)-κB is essential for tumour necrosis factor α (TNF-α) and nitric oxide production, we further investigated the effects of these possible EDCs on bacterial component-induced activation of NF-κB and found that reduced NF-κB activity is partly involved in the inhibition of TNF-α and nitric oxide production (Igarashi *et al.*, 2006). It is well known that lipopolysaccharide activates both MyD88-dependent and MyD88-independent pathways, and both signaling pathways are involved in lipopolysaccharide-induced production of TNF-α and nitric oxide (Akira & Takeda, 2004). The activation of both pathways leads to the activation of NF-κB, while the activation of the IFN-β promoter is induced only by the MyD88-independent pathway. Thus, to assess the influence of EDCs on the lipopolysaccharide-mediated MyD88-independent pathway, in the present study we have investigated the effects of possible

EDCs on lipopolysaccharide-induced activation of the IFN-β promoter. The chemicals were selected from the SPEED'98 list (http://www.env.go.jp/en/chemi/ed.html; SPEED'98 has been revised and 'Perspectives on Endocrine Disrupting Effects of Substances – ExTEND 2005' has been issued during the preparation of this manuscript) issued by the Ministry of the Environment of Japan depending on their availability and water solubility. Chemicals showing higher cellular toxicity were excluded. We selected 37 chemicals (described as EDCs in this study) that are suspected of having endocrine-disrupting effects from among agrochemicals and resin-related chemicals, and their abbreviations are shown in Table 1. We used the mouse macrophage cell line RAW 264, stably carrying an IFN-β-dependent luciferase reporter gene, to systematically compare the effect of each chemical on lipopolysaccharide-induced activation of the MyD88-independent pathway. Cells were incubated with 100 μM of each chemical followed by lipopolysaccharide, and then the reporter activity was measured. The reporter activity was normalized to the protein concentration for the compensation of difference in cell numbers and viabilities between wells. Table 1 summarizes the results. Seventeen chemicals: ACL, ATZ, BML, BPA, NAC, DEP, DPrP, KLT, KPN, MAT, DMDT, OCS, PCP, NNP, OTP, CAT and ZRM, inhibited lipopolysaccharide-induced activation of the IFN-β promoter. A strong inhibitory effect was observed with KPN and ZRM. No significant enhancement of lipopolysaccharide-induced activation of the IFN-β promoter was observed with any of the chemicals. We next examined the concentration dependency of the 16 chemicals that affected lipopolysaccharide-induced activation of IFN-β (Fig. 1). The effects of CAT could not be evaluated because of its poor solubility. Although the effects of OCS, DEP and DprP were weak even at 200 μM, all of the EDCs tested inhibited the activation in a concentration-dependent manner.

In the present study, we examined the effects of 37 chemicals suspected of having endocrine-disrupting properties on lipopolysaccharide-induced activation of the IFN-β promoter, to evaluate the effect of EDCs on macrophage activation. We found that 17 of the chemicals inhibited IFN-β promoter activation (Table 1). No chemicals by themselves induced IFN-β promoter activation nor enhanced lipopolysaccharide-induced activation. In this study, the chemicals we examined are classified as agrochemicals and resin-related chemicals. We found that stronger inhibitory activity was observed with agrochemicals. Most of the chemicals showed their effects at a concentration range of 50–200 μM, which may be higher than the levels that typically occur in the environment. In the natural environment, humans are exposed to multiple chemicals chronically, and the bioaccumulation and synergistic effects of these chemicals are not well understood; therefore, it may be possible that chronic exposure to even low levels of these chemicals could have some impact on human health.

Table 1. Effects of possible EDCs on lipopolysaccharide-induced activation of IFN-β promoter

Chemicals	Abbreviation	Class	% Response
Alachlor	ACL	a	43.5 ± 3.91**
Aldicarb	ACB	a	104.9 ± 2.38
Amitrole	ATA	a	92.3 ± 6.20
Atrazine	ATZ	a	49.3 ± 5.93*
Benomyl	BML	a	34.7 ± 6.31
Benzophenone	BZP	r	84.1 ± 7.31
Butyl benzyl phthalate	BBP	r	104.8 ± 10.64
Bisphenol A	BPA	r	59.2 ± 5.57*
Carbaryl	NAC	a	78.0 ± 6.99*
2,4-Dichlorophenoxy acetic acid	2,4-D	a	109.8 ± 15.90
Dibutyl phthalate	DBP	r	99.7 ± 5.23
2,4-Dichlorophenol	DCP	r	74.4 ± 6.34
Dicyclohexyl phthalate	DCHP	r	98.3 ± 18.46
Diethylhexyl adipate	DOA	r	80.5 ± 4.69
Diethylhexyl phthalate	DOP	r	82.5 ± 4.70
Diethyl phthalate	DEP	r	62.9 ± 7.04*
Dihexyl phthalate	DHP	r	81.0 ± 4.15
Di-*n*-pentyl phthalate	DPP	r	82.2 ± 9.60
Dipropyl phthalate	DPrP	r	72.4 ± 1.86**
Kelthane	KLT	a	30.7 ± 6.24**
Kepone	KPN	a	5.2 ± 0.54**
Malathion	MAT	a	73.6 ± 4.45*
Methomyl	MTM	a	96.1 ± 7.96
Methoxychlor	DMDT	a	81.5 ± 2.08*
Metribuzin	MTB	a	86.3 ± 5.23
Nitrofen	NIP	r	104.0 ± 6.16
4-Nitrotoluene	NTT	r	111.7 ± 4.90
Octachlorostyrene	OCS	r	77.2 ± 1.59**
Pentachlorophenol	PCP	a	61.4 ± 4.80**
Nonyl phenol	NNP	r	52.8 ± 2.61**
p-Octylphenol	OTP	r	56.4 ± 1.08**
Permethrin	PMT	a	100.1 ± 7.86
Simazine	CAT	a	72.9 ± 1.40**
Trifluralin	TFR	a	87.2 ± 5.22
2,4,5-Trichlorophenoxyacetic acid	2,4,5-T	a	94.6 ± 5.13
Vinclozolin	VCZ	a	87.4 ± 5.64
Ziram	ZRM	a	0.2 ± 0.09**

Values are expressed as percent (mean ± SEM) of respective control where no EDC treatment was performed. Data are from at least three independent experiments. All chemicals were used at 100 mM.

*$P < 0.05$.

**$P < 0.01$, compared with the respective control by paired Student's *t*-test.

a, Agrochemicals; r, resin-related chemicals.

We previously reported (Hong *et al.*, 2004; Igarashi *et al.*, 2006) that ACL, NAC, CAT, NNP and OTP, which inhibited either lipopolysaccharide-induced TNF-α or nitric oxide production by macrophages, also inhibited lipopolysaccharide-induced NF-κB activation. In the present study, we found that these chemicals also inhibit lipopolysaccharide-

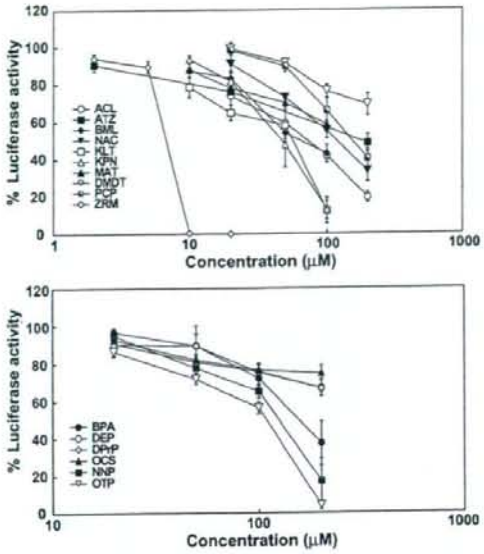

Fig. 1. Concentration-dependent effects of possible EDCs on lipopolysaccharide-induced activation of the IFN-β promoter. RAW 264 cells stably carrying an IFN-β-dependent luciferase reporter gene were stimulated with 10 ng mL^{-1} of lipopolysaccharide for 6 h with or without the indicated concentrations of EDCs, and luciferase activity was then measured. Values are means ± SEM from at least three independent experiments. The reporter activity in response to lipopolysaccharide alone is expressed as 100%.

induced IFN-β promoter activity. Since both MyD88-dependent and MyD88-independent pathways are essential for the production of TNF-α and nitric oxide, the inhibition of both NF-κB and IFN-β promoter activity by these chemicals may be involved in the inhibitory effects on TNF-α and nitric oxide production. Most, but not all, of the chemicals that inhibited lipopolysaccharide-induced IFN-β promoter activity also possessed inhibitory activity on lipopolysaccharide-induced NF-κB activation (Igarashi *et al.*, 2006). ACL and NAC, even at 370 and 500 μM, respectively, did not significantly affect SV40 promoter-based reporter activity (data not shown), indicating that the effect of these chemicals on IFN-β promoter and NF-κB activity was not non-specific. Although the mechanism by which these chemicals inhibit both activities is unknown, activation of NF-κB and stimulation of MyD88-independent signaling are essential to the innate immune function. It is, therefore, of concern that these chemicals may have the potential to exacerbate infectious diseases.

Acknowledgement

This work was supported in part by a grant from the Ministry of the Environment, Japan.

References

Akira S & Takeda K (2004) Toll-like receptor signalling. *Nat Rev Immunol* **4**: 499–511.

Eskenazi B, Mocarelli P, Warner M, Samuels S, Vercellini P, Olive D, Needham L, Patterson D & Brambilla P (2000) Seveso Women's Health Study: a study of the effects of 2,3,7,8-tetrachlorodibenzo-*p*-dioxin on reproductive health. *Chemosphere* **40**: 1247–1253.

Fujihara M, Muroi M, Tanamoto K, Suzuki T, Azuma H & Ikeda H (2003) Molecular mechanisms of macrophage activation and deactivation by lipopolysaccharide: roles of the receptor complex. *Pharmacol Ther* **100**: 171–194.

Hong CC, Shimomura-Shimizu M, Muroi M & Tanamoto K (2004) Effect of endocrine disrupting chemicals on lipopolysaccharide-induced tumor necrosis factor-alpha and nitric oxide production by mouse macrophages. *Biol Pharm Bull* **27**: 1136–1139.

Igarashi A, Ohtsu S, Muroi M & Tanamoto K (2006) Effects of possible endocrine disrupting chemicals on bacterial component-induced activation of NF-kappaB. *Biol Pharm Bull* **29**: 2120–2122.

Inoshita H, Masuyama H & Hiramatsu Y (2003) The different effects of endocrine-disrupting chemicals on estrogen receptor-mediated transcription through interaction with coactivator TRAP220 in uterine tissue. *J Mol Endocrinol* **31**: 551–561.

Masuyama H, Hiramatsu Y, Kunitomi M, Kudo T & MacDonald PN (2000) Endocrine disrupting chemicals, phthalic acid and nonylphenol, activate Pregnane X receptor-mediated transcription. *Mol Endocrinol* **14**: 421–428.

Safe S, Wang F, Porter W, Duan R & McDougal A (1998) Ah receptor agonists as endocrine disruptors: antiestrogenic activity and mechanisms. *Toxicol Lett* **102–103**: 343–347.

Schrenk D (1998) Impact of dioxin-type induction of drug-metabolizing enzymes on the metabolism of endo- and xenobiotics. *Biochem Pharmacol* **55**: 1155–1162.

Food Additives and Contaminants, August 2007; 24(8): 799–806

Taylor & Francis
Taylor & Francis Group

Quantitative nuclear magnetic resonance spectroscopic determination of the oxyethylene group content of polysorbates

NAOKI SUGIMOTO[1], RYO KOIKE[2], NORIKO FURUSHO[1], MAKOTO TANNO[2], CHIKAKO YOMOTA[1], KYOKO SATO[1], TAKESHI YAMAZAKI[1], & KENICHI TANAMOTO[1]

[1]*National Institute of Health Sciences: 1-18-1, Kamiyoga, Setagaya, Tokyo 158-8501, Japan and* [2]*Kao Corporation, Analytical Research Center, 1334, Minato, Wakayama-shi, Wakayama 640-8580, Japan*

(Received 30 November 2006; revised 5 February 2007; accepted 13 February 2007)

Abstract
Guidelines for the oxyethylene group (EO) content of polysorbates are set by the Food and Agriculture Organization/World Health Organization Joint Expert Committee on Food Additives. However, the classical titration method for EO determination is difficult and time-consuming. Here, we show that quantitative ^{1}H-nuclear magnetic resonance spectroscopy can determine the EO contents of polysorbates rapidly and simply. The EO signals were identified through comparisons with sorbitan monolaurate and poly(ethylene glycol) distearate. Potassium hydrogen phthalate was used as an internal standard. The EO contents were estimated from the ratio of the signal intensities of EO to the internal standard. Two nuclear magnetic resonance systems were used to validate the proposed method. The EO content of commercial polysorbates 20, 60, 65, and 80 was determined to be within the recommended limits using this technique. Our approach thus represents an additional or alternative method of determining the EO contents of polysorbates.

Keywords: *Analytical method, food additive, oxyethylene, polysorbate, quantitative nuclear magnetic resonance*

Introduction

Polysorbates are non-ionic surfactants that are widely used as emulsifiers, dispersants, and stabilizers in food processing. Polysorbates consist of a mixture of fatty-acid partial esters of sorbitol and condensed sorbitol anhydrides, and contain approximately 20 moles of ethylene oxide (comprising the oxyethlene unit [EO] $-OC_2H_4-$) for each mole of sorbitol, along with its monohydrides and dianhydrides. The main fatty acids of polysorbates 20, 60, 65, and 80 are monolauric acid, monostearic acid, tristearic acid, and monooleic acid, respectively. The typical structures of these polysorbates are shown in Figure 1.

Guidelines for the EO contents of polysorbates are set by the Food and Agriculture Organization (FAO)/World Health Organization (WHO) Joint Expert Committee on Food Additives (JECFA). To comply with the JECFA standards, the quality and composition of commercially synthesized polysorbates must be monitored and regulated. The standard method of measuring EO as described in "section VI. Methods for fats and related substances in the guide to specification" is as follows: "The oxyethylene groups are converted to ethylene and ethyl iodide which can be determined by titration. By utilizing a conversion factor determined on a reference sample, it is possible to compute the polyoxyethylene ester content" (JECFA [internet]). However, this classical titration method requires a complicated apparatus and involves several time-consuming steps. Alternative methods for determining the EO contents of polysorbates have not previously been reported, because these complex compounds are mixtures of isomers that are non-selectively substituted with EOs and fatty acids.

The quantitative nuclear magnetic resonance (qNMR) approach is based upon the International

Correspondence: Naoki Sugimoto. E-mail: nsugimot@nihs.go.jp

ISSN 0265-203X print/ISSN 1464-5122 online
DOI: 10.1080/02652030701278347

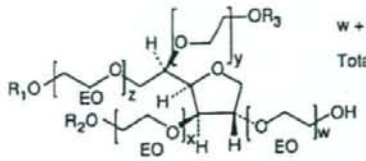

Compound			Formula (MW)	EO(%) in molecule
Polysorbate 20 (polyoxyethylene (20) sorbitan monolaurate)	R_1= 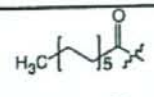	$R_2 = R_3 = H$	$C_{58}H_{114}O_{26}$ (MW1227.5)	EO(%) = 71.8
Polysorbate 60 (polyoxyethylene (20) sorbitan monostearate)	R_1= 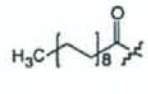	$R_2 = R_3 = H$	$C_{64}H_{126}O_{26}$ (MW1311.7)	EO(%) = 67.2
Polysorbate 65 (polyoxyethylene (20) sorbitan tristearate)	$R_1 = R_2 = R_3 =$ 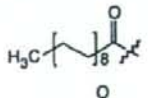		$C_{100}H_{194}O_{28}$ (MW1844.6)	EO(%) = 47.8
Polysorbate 80 (polyoxyethylene (20) sorbitan monooleate)	R_1= 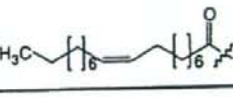	$R_2 = R_3 = H$	$C_{63}H_{122}O_{26}$ (MW1295.6)	EO(%) = 68.0

Figure 1. Typical structures of polysorbates 20, 60, 65, and 80. The formulae and EO (%) were estimated based on the assumption that there were 20 moles of EO per molecule.

system of units (SI units). This valuable technique meets the requirements of a primary ratio analytical method (Jancke 1998). The use of qNMR to determine the ethanol content of deuterium oxide solution was previously reported as a part of an intercomparison study organized by the Comité Consultatif pour la Quantité de Matère (CCQM). The results showed that the accuracy of qNMR was equivalent to that of gas chromatography with a flame ionization detector (GC-FID) (Saito et al. 2003). qNMR exploits the fact that the signal intensities of a given NMR resonance are directly proportional to the molar amount of the nucleus within the sample. qNMR can determine the quantity of a compound, its substituent contents, or its absolute quality if the whole sample weight is known. This technique has several advantages for the analysis of organic compounds: it is non-destructive, it provides both quantitative data and structural information about a compound, and high-throughput spectral-acquisition instruments are commercially available. The main drawback of the qNMR approach is that manual spectral assignment is required; however, this can easily be rectified by applying current NMR technical experiments such as total correlated spectroscopy (TOCSY), heteronuclear multiple quantum correlation (HMQC), heteronuclear multiple bond coherence (HMBC), etc.

Based on these features of qNMR, we predicted that the method could be used to determine the EO contents of polysorbates. In the current paper, we detail the application of qNMR along with an internal standard for the direct determination of the EO contents of polysorbates.

Materials and methods

Materials

Samples of reagent-grade polysorbates 20, 60, 65, 80, and sorbitan monolaurate (Span 20) were purchased from Wako Pure Chemical Industries, Ltd (Osaka, Japan). Poly(ethylene glycol) distearate was purchased from Sigma-Aldrich Japan KK (Tokyo). Commercial samples of polysorbates were obtained from companies A–E via the Japan Food Additives Association. The NMR solvents, methanol-d_4 and acetone-d_6 with 0.03% tetramethylsilane (TMS), were purchased from Isotec Inc. (Miamisburg, OH). Potassium hydrogen *phthalate* (PHP), which was standard grade for volumetric analysis according to Japanese Industrial Standard (JIS) K8005, was purchased from Wako Pure Chemical Industries, Ltd.

Instrumentation

NMR spectra were recorded on JNM-ECA (500 MHz; JEOL, Tokyo) and MERCURY (400 MHz; VARIAN, Palo Alto, CA) pulsed Fourier-transform (FT) spectrometers, equipped with 5 mm $^1H\{X\}$ inverse detection gradient

Table I. Instruments and acquisition parameters.

Spectrometer	MERCURY400 (VARIAN) and ECA500 (JEOL)
Probe	5 mm indirect detection probe
Spectral width	2.5–12.5 ppm
Data points	64 000
Flip angle	45°
Pulse delay	30 s (>5 * T_1)
Scan times	8
Sample spin	15 Hz
Probe temperature	25°C
Solvent	Mixture of methanol-d_4 and acetone-d_6 (1:1)
Internal standard	Potassium hydrogen phthalate (PHP)
Range of integral signal	Oxyethylene group (EO) = 3.40–3.85 ppm 4 protons of PHP = 7.46–7.66 ppm + 8.18–8.38 ppm

probes, with methanol-d_4:acetone-d_6 (1:1) and 0.3% (w/v) PHP as an NMR solvent. The spectra were referenced internally to TMS by ^{1}H-NMR. The samples and internal standard were weighed on a LIBROR AEG-80SM (Shimadzu, Kyoto, Japan) electronic balance to an accuracy of ±0.01 mg.

Preparation of samples and NMR measurement conditions

The polysorbate samples were prepared as follows. PHP was crushed into a powder in a mortar and dried for 1 h at 120°C. After cooling in a desiccator, the powder (300 mg) was dissolved in 100 ml of methanol-d_4:acetone-d_6 (1:1) with ultrasonic agitation for 30 min. This stock solution was used as the NMR solvent and included an internal standard. A 50-mg polysorbate sample was then dissolved in 3 ml of the NMR solvent described above, and 0.6 ml of the sample solution was placed into a 5-mm NMR tube (Kusano Science Co. Ltd, Tokyo). The ^{1}H-NMR spectra were recorded on MERCURY400 and ECA500 spectrometers operating at 400 and 500 MHz, respectively. Typical ^{1}H-NMR parameters for the quantitative analyses are listed in Table I. The free induction decay (FID) signals of the samples from the MERCURY400 and ECA500 spectrometers were loaded onto a Windows XP-based personal computer (PC) equipped with the Alice 2 Version 5 (JEOL) NMR data-processing and analytical software. Fourier transformations of the FID signals were carried out with this software using the default parameters; window function = exponential, BF = 0.12 Hz, zero filling = 1, T1 = T2 = 0%, T3 = 90%, T4 = 100%. After phase adjustments and baseline corrections of the NMR spectra were performed using the same algorithms in the automatic mode of Alice 2, the signal intensities of the EOs and internal standard protons were measured, respectively.

Results and discussion

Identification of EO signals in polysorbates

Polysorbate molecules contain approximately 20 moles of EO according to the JECFA definition. However, recently reported matrix-assisted laser desorption/ionization time-of-flight mass spectrometry (MALDI-TOF MS) spectra showed that polysorbates include numerous other chemical species, including polyethylenes, unesterified, monoesterified, and diesterified polyoxyethylene sorbitans, and isosorbides (Frison-Norrie and Sporns 2001). Furthermore, analysis by liquid chromatography (LC)–mass spectrometry (MS) confirmed that polysorbates contain not only polyoxyethylene sorbitan fatty acid esters but also numerous intermediates, such as polyoxyethylene sorbitan and isosorbitan, and the monoesters and diesters of fatty acids (Vu Dang et al. 2006). These studies have confirmed that polysorbates comprise many types of chemical isomers. This molecular diversity makes it difficult to determine the EO contents of polysorbates. However, we hypothesized that the EO contents of polysorbates could be measured rapidly and simply by qNMR if the signals could be identified on ^{1}H-NMR spectra, regardless of whether they contained numerous chemical isomers.

Thus, in order to identify the EO signals in polysorbates, we compared the ^{1}H-NMR spectra of polysorbate 20, sorbitan monolaurate, and poly(ethylene glycol) distearate. The partial structures of sorbitan monolaurate and poly(ethylene glycol) distearate, which comprised a sorbitol anhydride core and poly(ethylene glycol), were similar to those of polysorbate 20 (Figures 2 and 3). The sorbitan monolaurate and poly(ethylene glycol) distearate spectra revealed fatty-acid moiety signals with δ_H values ranging from 0.9 to 2.4 ppm, similar to those of polysorbate 20. The triplet signal at δ_H *c.* 0.9 ppm, the major broad signal and multiplet signal at δ_H *c.* 1.3 ppm and 1.6 ppm, and the triplet signal at δ_H *c.* 2.4 ppm were identified as the terminal CH_3–, $-CH_2-$, and $-CH_2C{=}O-$ groups of the fatty acids, respectively. Most of the EO signals in poly(ethylene glycol) distearate were observed between δ_H values of 3.40 and 3.85 ppm. One of the $-CH_2O-$ groups appeared to have been shifted downfield to δ_H *c.* 4.2 ppm, near to the residual proton of methanol-d_4 at δ_H *c.* 4.4 ppm. A HMBC experiment revealed that the proton at δ_H *c.* 4.2 ppm was correlated to the carbonyl carbon of the fatty acid at δ_C 173.4 ppm. Thus, the proton signal was assigned

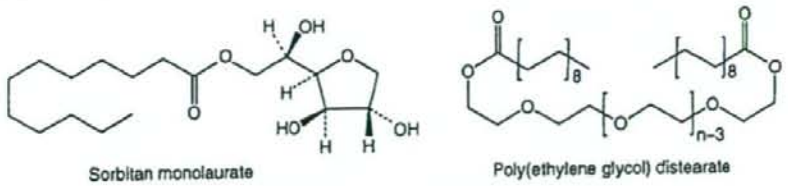

Figure 2. Structures of sorbitan monolaurate and poly(ethylene glycol) distearate.

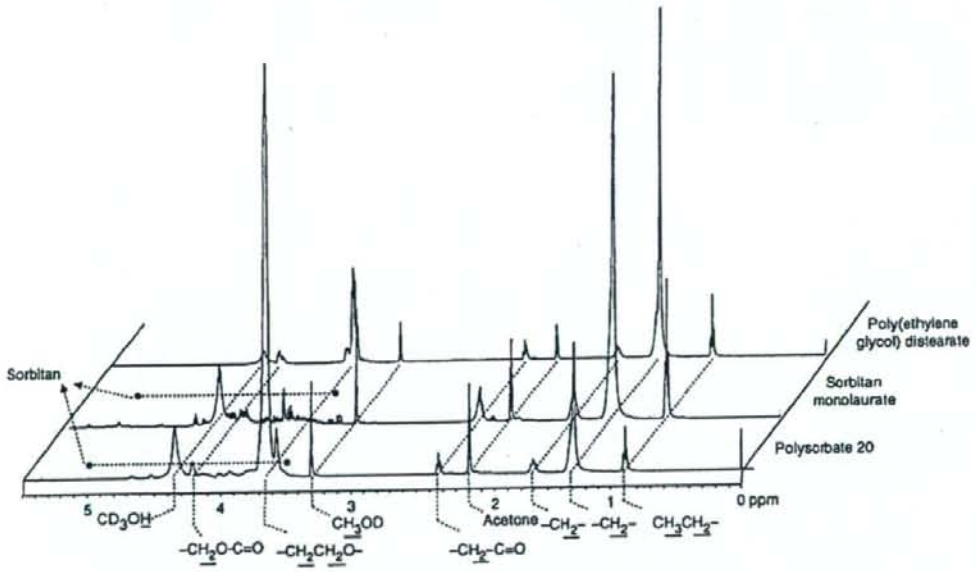

Figure 3. Comparison of NMR spectra of polysorbate 20, sorbitan monolaurate and poly(ethylene glycol) distearate. ^{1}H-NMR spectra were obtained using the ECA500 system (500 MHz; JEOL) under the conditions shown in Table I.

to the $-CH_2O-$ group adjacent to the fatty acid side chain. In the sorbitan monolaurate spectrum, various minor proton signals were observed from δ_H values of *c.* 3.4–5.0 ppm; these were attributed to the sorbitan moiety in sorbitan monolaurate, which consists of a mixture of cyclic sorbitol-derived ethers (such as sorbitan, isosorbite, and other isomers). These signals were also observed on the spectrum of polysorbate 20. However, the signals were broad and negligibly smaller than that of sorbitan monolaurate, as polysorbate 20 has the diversity of molecule more than sorbitan monolaurate. The polysorbate 20 signals ranging from δ_H 0.9 to 2.4 ppm that were attributed to the fatty-acid moiety were similar to those of sorbitan monostearate and poly(ethylene glycol) distearate. Polysorbate 60, 65, and 80 also showed the signals of fatty acid as same as sorbitan monolaurate, but the olefinic protons were only observed at δ_H 5.3 ppm on the spectrum of polysorbate 80 consisting of an unsaturated fatty acid (data not shown). The EO signals were assigned to a large envelop between δ_H 3.40 and 3.85 ppm, and at δ_H 4.20 ppm, which overlapped with the negligible small broad signals seen for the mixture of sorbitan, isosorbite, and other isomers moieties between δ_H values of *c.* 3.4 and 5.0 ppm. The EO signals of polysorbates 60, 65, and 80 also appeared within these ranges (data not shown). This was due to the fact that polysorbates basically comprise the same units: sorbitol anhydrides core, EO chains, and fatty acids. Although proton signals of the $-CH_2O-$ group adjacent to the fatty acid at δ_H *c.* 4.20 ppm were observed, and the signals of the sorbitol anhydrides core were overlapped on EO signals, they were negligible and did not effect the